Understanding the Optical Band Shape: Coumarin-153 Steady-State Spectroscopy

Dmitry V. Matyushov*,† and Marshall D. Newton*,‡

Department of Chemistry and Biochemistry, Arizona State University, P.O. Box 871604, Tempe, Arizona 85287-1604, and Brookhaven National Laboratory, Chemistry Department, Box 5000, Upton, New York 11973-5000

Received: March 22, 2001; In Final Form: July 10, 2001

We have developed a band-shape analysis of optical transitions in polarizable chromophores characterized by large magnitudes of the transition dipole (intense transitions). The model is tested on steady-state spectra of the coumarin-153 optical dye, employing an explicit solvent description accounting for dipole moment, quadrupole moment, and polarizability of the solvent molecules. The calculations are performed for solvents ranging from nondipolar to strongly dipolar. The solvent dependence of both the experimental Stokes shift and the spectral width is satisfactorily reproduced over the whole polarity range. The optical width is shown to demonstrate a qualitatively different solvent dependence for absorption and emission. The solvent-induced absorption width increases with solvent polarity, whereas the solvent-induced emission width passes through a maximum. This is a result of non-Gaussian statistics of the energy gap fluctuations in polarizable/electronically delocalized chromophores. The total (i.e., solvent and vibrational) emission width tends to pass through a broad maximum at low solvent polarities, decreasing with solvent polarity for highly polar solvents. This results from the combined influence of a solvent-induced mixing of the vacuum adiabatic states and a decrease of the vibrational reorganization energy with increasing solvent polarity. The latter effect arises as a result of a coupling of the vibrational and solvent nuclear modes due to the electronic state occupation number difference, making the vibrational reorganization energy solvent-dependent. The study revels a breakdown of the linear relation between the solvent-induced width and Stokes shift. The model suggests that the Franck−Condon factor of intense optical lines should significantly depend on the magnitude of the transition dipole.

1. Introduction

Shifts of optical lines in condensed phases reflect the overall solvation power of the solvent produced by various types of solute−solvent interactions. Each component of the total interaction potential reflects some specific solvent property, electrostatic or nonelectrostatic in nature, with a characteristic relaxation time. The vertical Franck−Condon (FC) transition of an optical excitation[1] separates the overall solvation energy into the components generated by the solvent modes that are fast and slow compared to the characteristic time scale of the transition.[2] Two general classes of solvent excitations, associated with the electronic and nuclear degrees of freedom, are usually considered. They result in, correspondingly, the electronic and nuclear components of the spectral shift. Electronic solvation, responsible for dispersion and induction interaction potentials, may account for a considerable portion of the solvent-induced spectral shift, especially in weakly polar and nondipolar solvents.[3] Nuclear solvation, arising from permanent electrical moments (e.g., modeled by fixed partial charges on the solvent molecules), is more important in polar solvents.

Regardless of its quantitative significance for a particular process, solvation by the solvent nuclear degrees of freedom is the key driving force of many condensed phase nonequilibrium phenomena such as solvation dynamics[4a] and radiationless transitions.[4b,c] Understanding of energetics and dynamics of nuclear solvation is therefore crucial for these applications. The present study is a step toward better understanding of the energetics of nuclear solvation and reorganization in liquid solvents experimentally probed by band shapes of steady-state optical spectra and activation barriers of charge transfer (CT) reactions. In the remainder of the paper, the focus is primarily on the "electron transfer" (ET) subset of CT processes, in which the degree of CT is characterized by state occupation numbers n (populations) defined in terms of a reference basis taken as the vacuum adiabatic states.[5,6] ET traditionally refers to the situation in which the activation energetics can be calculated as if a full electron is transferred in the process (i.e., $\Delta n = 1$[5,6]), even though, strictly speaking, due to nonzero electronic overlap, the actual population shift may be appreciably less than unity. We use the term CT to indicate that in the processes studied here the solvent-induced mixing of the initial and final states and partial transfer of the electronic density do affect the FC factors of optical and thermal transitions.

The thermodynamic strength of nuclear solvation is traditionally related to the solvent reorganization energy λ_s of optical transitions or CT reactions.[7] This parameter reflects the free energy invested in achieving the resonance of electronic states for thermal transitions and the bandwidth of inhomogeneously broadened lines[8] for optical transitions. Steady-state optical spectroscopy is a principal experimental source of the reorganization energies. The isomorphism between optical band shapes and FC factors entering rate constants of thermally activated transitions[9] establishes a connection between optical CT bands[10] and rates of CT reactions.[11] Therefore, both band-shape analysis

* Corresponding authors.
† Arizona State University. E-mail: dmitrym@asu.edu.
‡ Brookhaven National Laboratory. E-mail: newton@bnl.gov.

10.1021/jp011074f CCC: $20.00
Published on Web 08/28/2001

and modeling of redox reactions in solution present a need for an accurate and reliable account of the key factors influencing nuclear reorganization.[12]

Two observables are commonly extracted from optical spectra: the first and second spectral moments. Both provide information about the solvent reorganization energy. The Marcus−Hush model of CT transitions[9] relates the spectroscopic Stokes shift to the total nuclear reorganization energy of the system

$$2(\lambda_s + \lambda_v) = \Delta\bar{\nu}_{st}, \qquad \Delta\bar{\nu}_{st} = \bar{\nu}_{abs} - \bar{\nu}_{em} \tag{1}$$

where $\bar{\nu}_{abs}$ and $\bar{\nu}_{em}$ stand for the first spectral moments of absorption ("abs") and emission ("em") lines; all energy parameters appearing below are in wavenumbers (cm^{-1}). The intramolecular reorganization energy λ_v arises as a result of displacements of solute vibrational modes caused by the electronic transition. The vibronic band including the effects of solvent and intramolecular vibrations is then formed as a superposition of individual Gaussian lines created by a statistical distribution of solvent configurations (inhomogeneous broadening).[10]

The second spectral moments[13] of absorption and emission lines, $\langle(\delta\bar{\nu})^2\rangle_{abs/em}$, are equal to each other in the Marcus−Hush formalism[14]

$$\langle(\delta\bar{\nu})^2\rangle_{abs} = \langle(\delta\bar{\nu})^2\rangle_{em} \tag{2}$$

They are related to the solvent and intramolecular reorganization energies of the optical chromophore as follows:[9b]

$$\langle(\delta\bar{\nu})^2\rangle_{abs/em} = 2k_BT\lambda_s + \bar{\nu}_v\lambda_v \tag{3}$$

where $\bar{\nu}_v$ is a characteristic frequency of intramolecular vibrations. Together, eqs 1 and 3 result in the fundamental relation between the Stokes shift and the spectral width

$$\beta\langle(\delta\bar{\nu})^2\rangle_{abs/em} = \Delta\bar{\nu}_{st} + \lambda_v(\beta\bar{\nu}_v - 2) \tag{4}$$

where $\beta = 1/k_BT$ (in cm).

Equation 4 provides a direct connection between the first and second spectral moments, reflecting some fundamental assumptions of the Marcus−Hush model of ET that can be summarized as follows. (1) A two-state solute is adopted (i.e., no excitations to higher electronic states are included). (2) Neglecting electronic coupling between the two states participating in the transition, given by the off-diagonal Hamiltonian matrix element for thermal transitions[15] and by the transition dipole for optical transitions, in defining the FC factors of optical and thermal ET. (3) Decoupling of the vibrational and solvent nuclear modes. (4) Linear solvent response: the reaction field induced by the solute in the solvent is a linear function of solute's charge distribution.

Equations 2 and 4 give two predictions that can be verified experimentally. First (eq 2), the width of the absorption line is equal to the width of the corresponding emission line. Second (eq 4), both the absorption and emission widths are linear functions of the Stokes shift with unit slope. There are, however, several indications in the literature that both these features can be dramatically violated for some optical dyes. The widths of absorption lines are sometimes substantially different from the widths of emission lines.[16,17] Furthermore, the progression of the spectral widths with solvent polarity can be dramatically different for absorption and emission, resulting in distinctly different slopes when plotted against the Stokes shift. An illuminating example of such a behavior is spectroscopy of coumarin-153 (C153) dye, shown in Figure 1 (data according to Reynolds et al[18]). The spectral width $\sigma_{abs/em}$ in Figure 1 is obtained from the half-intensity width $\Gamma_{abs/em}$ as

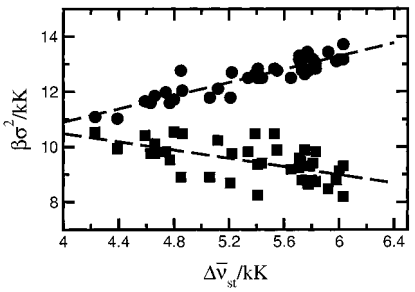

Figure 1. Absorption (circles) and emission (squares) widths (eq 5) vs the Stokes shift for 40 molecular solvents according to Reynolds et al.[31] The dashed lines are regressions drawn as a guide for the eye.

$$\sigma_{abs/em}{}^2 = (\Gamma_{abs/em}{}^2)/(8 \ln 2) \tag{5}$$

The most puzzling feature is the opposite slopes of the absorption and emission progressions of the width versus the Stokes shift. The polarity decay of the emission width for C153 is not clearly supported by the data from other laboratories (see Results below). Nevertheless, it seems to be fairly well established in the literature that the solvent progression of the width may be different for emission and absorption bands.[19] The present work is a step toward better understanding of this phenomenon.

In view of considerable deviations of the observed optical widths from the prediction of the Marcus−Hush model (eqs 2 and 4), one can raise the question as to which of the above-mentioned assumptions 1−4 are violated. The linear response approximation (LRA, assumption 4) in applications to ET reactions,[20] solvation dynamics,[21] and optical spectra[22] has been extensively tested on computer simulations and analytical solvation theories. Although some deviations from nonlinearity are indeed seen for solid media,[23] protonated solvents,[24] and supercritical solvation,[25] the nonlinear solvation effect is generally small for large chromophores in dense liquid solvents. The other assumptions of the Marcus−Hush description, eqs 1−3, need, however, closer scrutiny.

The omission of the effect of transition dipole on the FC factor (assumption 2) can be justified only if the two states involved in the transition do not mix under the influence of the nuclear fluctuations in the system. Both in the adiabatic and diabatic representations, this is achieved at zero transition dipole moment.[5,26,27] The analysis of optical band shapes in a two-state model, in which the vacuum adiabatic states are mixed by the adiabatic transition dipole $m_{0,12}$, shows that the emission width is smaller than the absorption width.[5] Furthermore, the emission width decays, and the absorption width increases when plotted against the Stokes shift, in qualitative agreement with the picture shown in Figure 1. Despite this qualitative agreement, the two-state model (TSM, assumption 1) is very unrealistic due to the neglect of excited electronic states of the chromophore, leading, for instance, to a negative excited state polarizability. The polarizability of the excited state of essentially all known chromophores is, on the contrary, positive and in the majority of cases is higher than that of the ground state. This is the case for the C153 optical dye.[28] Finally, the decoupling of the solvent and vibrational nuclear modes (assumption 3) breaks down when the electronic density is

delocalized. The coupling of the electron to intramolecular vibrations is proportional to the occupation number of the corresponding electronic state,[17] which in turn may be changed by the fluctuating solvent nuclear field.

Another interesting problem raised by steady-state spectroscopy of C153[18] is that of the role of nondipolar solvation in solvent reorganization. The traditional continuum dielectric models of solvent reorganization in optical and thermal electronic transitions are intended for use with dipolar media, yielding a virtually vanishing solvent reorganization energy, $\lambda_s \propto (1/\epsilon_\infty - 1/\epsilon_s)$, in nondipolar solvents (zero permanent dipole moments), with the static dielectric constant ϵ_s very close to the high-frequency dielectric constant ϵ_∞.[7] On the other hand, recent applications of the optical band-shape analysis to intramolecular optical transitions in chromophores dissolved in nondipolar solvents yield classical reorganization energies of appreciable magnitude ($\lambda_{cl} = 0.1 - 0.4$ eV).[11] Combined application of the band-shape analysis and Raman spectroscopy[30] allows separation of the low-frequency solute vibrational and solvent components of the overall classical reorganization energy. This analysis demonstrates a substantial solvent component, λ_s, in λ_{cl}.[30b-d] A considerable solvent component in the classical reorganization energy in nondipolar solvents is also observed in Stokes shift measurements of C153[31] and a more recent study on a donor-bridge-acceptor molecule.[32] The solvent component of the Stokes shift is distinctly nonzero (about 0.08 eV for C153 in benzene), underscoring the fact that the continuum cavity models are not appropriate for treating solvation in nondipolar solvents.

A nonzero reorganization energy in some nondipolar solvents has been attributed to solvation by solvent quadrupoles.[31] Despite the fact that the importance of higher multipoles is currently accepted in the literature,[33,34] there is still insufficient understanding of the relative contribution of dipolar and quadrupolar components to the overall nuclear solvent reorganization. To explore this issue, we apply here a recently developed perturbation approach to equilibrium solvation in dipolar−quadrupolar solvents[35] to model the solvent dependence of the Stokes shift. This approach explicitly separates the dipolar and quadrupolar components of solvation, a capability which is not available in other models.[34]

The model proposed in this study includes several features that are significant for a correct description of optical band shapes: (1) Delocalization of the electronic density between the two states participating in the transition and coupled by a transition dipole. (2) Solute polarizability due to the solute's excited states other than the two states participating in the transition. (3) Microscopic modeling of the solvent-induced Stokes shift, including both dipolar and quadrupolar solvation mechanisms. (4) Coupling of the solvent and vibrational nuclear modes, making the vibrational solvent reorganization energy solvent-dependent. The theoretical procedure incorporates two previously considered limiting cases: the spectral analysis of the TSM,[5] which excludes excitations to higher-lying electronic states, and the theory of diabatic optical transitions in polarizable chromophores (referred to as diabatic polarizable model, DPM),[29] which omits electronic delocalization effects. The model developed here incorporates both delocalization and polarizability effects and will be referred to as the adiabatic polarizable model (APM). The theory is shown to reproduce satisfactorily the solvent polarity progression of both the Stokes shift and the widths of absorption and emission bands experimentally observed for C153. The calculation procedure is described in section 2. Results are given in section 3. Section 4 presents the discussion, and conclusions are outlined in section 5.

2. Calculation Procedure

2.1. Model. The goal of the present study is to develop an algorithm to calculate the alteration of optical band shapes induced by the solvent using the gas-phase chromophore parameters as an input. We use the optical bands measured experimentally in the gas phase and employ the solute parameters obtained from quantum-mechanical calculations. We start with a basis of two electronic states $\psi_i(\mathbf{r},\mathbf{Q}_0)$ ($i = 1, 2$) given as functions of electronic coordinates $\mathbf{r}$ at some configuration $\mathbf{Q}_0$ associated with normal vibrational modes of the solute $\mathbf{Q} = Q_1, ..., Q_N$ (crude adiabatic approximation[36]). The electronic transition alters the constants γ_{in} governing the electron−phonon coupling. This situation is represented by the standard electron−phonon Hamiltonian[1]

$$H_0 = \sum_{i=1,2}(E_i - \sum_n \gamma_{in}(Q_n - Q_{0n}))a_i^+ a_i + H_v \qquad (6)$$

with

$$H_v = \sum_n \left[\frac{\kappa_n(Q_n - Q_{n0})^2}{2} + T(Q_n)\right] \qquad (7)$$

Here, $T(Q_n)$ refers to the kinetic energy associated with the mode Q_n, κ_n is the vibrational force constant (taken as state-independent[14]), and a_i^+ and a_i are the fermionic creation and annihilation operators in the electronic states 1 and 2 involved in the transition. The energies E_i in eq 6 correspond to electronic states at the nuclear configuration $\mathbf{Q} = \mathbf{Q}_0$; the difference $\Delta E = E_2 - E_1$ is thus the gas-phase vertical absorption energy at $\mathbf{Q}_0$.

When the chromophore is placed in a solvent, the vibronic energies change as a result of solute−solvent interactions. For a dipolar solute, the interaction Hamiltonian is

$$H_{int} = -\hat{\mathbf{m}}_0 \cdot \mathbf{R} \qquad (8)$$

where $\hat{\mathbf{m}}_0$ is the solute dipole operator and $\mathbf{R}$ is the reaction field of the solvent, including the quantum field of electronic solvent polarization and a classical nuclear reaction field. If we confine the description to only two electronic states, the system Hamiltonian becomes

$$H = H_0 + H_{int} = \sum_{i=1,2}(E_i - \mathbf{m}_{0i}\cdot\mathbf{R} - \sum_n \gamma_{in} q_n)a_i^+ a_i - \mathbf{m}_{0,12}\cdot\mathbf{R}(a_1^+ a_2 + a_2^+ a_1) + H_v \qquad (9)$$

where $\mathbf{m}_{0,12} = \langle\psi_1|\hat{\mathbf{m}}_0|\psi_2\rangle$ is the gas-phase transition dipole, $\mathbf{m}_{0i} = \langle\psi_i|\hat{\mathbf{m}}_0|\psi_i\rangle$ is the gas-phase dipole moment in the ith state ($i = 1, 2$), and $q_n = Q_n - Q_{0n}$. The off-diagonal term here describes a solvent-induced non-Condon mixing between the states 1 and 2.[2d,e,5,37] The basis set of only two electronic states clearly does not provide a complete physical picture of the interaction of an optical chromophore with a condensed environment. Virtual electronic transitions to higher-lying states make a substantial addition to the polarizability of the two-state solute. Under the action of a solvent reaction field, the chromophore attains an induced dipole (higher induced multi-

poles are not considered here). For a complete modeling of the solvent-induced shift and broadening of the spectral line, one has to include both factors affecting the band shape: (i) direct delocalization of the electronic density between the two states participating in the transition[5] and (ii) virtual transitions to other excited states of the chromophore as part of the solute's polarizability response.[29] The importance of delocalization for modeling the spectral width has been recognized already in previous computational[37] and analytical[5] studies of optical spectra. A common approach adopted in computational modeling is to diagonalize the Hamiltonian matrix on the basis of a few electronic states for each solvent configuration generated by a molecular dynamics simulation.[37b] Polarizability converges very slowly as a function of the number of basis states.[38] Therefore, inclusion of only a few excited states may result in an incorrect polarizability and, consequently, incorrect account of the polarizability effects on the optical line-shape.

To incorporate correctly the chromophore polarizability on one hand and generate explicit electronic delocalization on the other, we adopt here a hybrid model. The two states participating in the transition are explicitly considered. Transitions to all other excited states of the chromophore are assumed to result in polarization of the electron density defined by the dipolar polarizability $\bar{\alpha}_{0i}$ ($i = 1, 2$). The total vacuum polarizability of the solute, treated as input available from experiment or independent calculations, is thus split into the polarizability from the $1 \leftrightarrow 2$ transition and the component $\bar{\alpha}_{0i}$ from all other transitions

$$\alpha_{0i}^{\alpha\beta} = \pm 2\frac{m_{0,12}^{\alpha}\, m_{0,12}^{\beta}}{\Delta E} + \bar{\alpha}_{0i}^{\alpha\beta} \tag{10}$$

Here, α and β superscripts refer to the Cartesian components of the transition dipole; "+" and "−" refer to $i = 1$ and $i = 2$, respectively.

The common situation for redox reactions and visible/UV spectra in solutions is that the frequency of electronic excitations of the solvent is much higher than the adiabatic energy gap between the ground and excited CT states of the solute. The induced solvent dipole moments (given by the electronic component of the solvent reaction field **R**) can then be integrated out to generate instantaneous CT free energy surfaces depending on the nuclear configuration of the system (i.e., constrained free energy surfaces depending on the instantaneous values of the nuclear coordinates).[2d,29] This approximation assumes adiabatic separation of the characteristic time scales of the optical transition and those of electronic excitations of the solvent.[2] We also assume that the solute electronic states responsible for $\bar{\alpha}_{0i}$ lie much higher in energy than the adiabatic states 1 and 2 participating in the transition. This assumption extends the adiabatic separation of electronic time scales to all induced dipoles in the system. This allows us to integrate out all the induced dipoles and define the instantaneous CT free energy depending on the nuclear configuration and occupations of states 1 and 2.[2d,6,29]

The effective Hamiltonian obtained by integrating out the induced dipole moments in the system depends on the nuclear configuration of the solvent solely through the nuclear reaction field $\mathbf{R}_p$[5]

$$\tilde{H} = \sum_{i=1,2} E_{0s}^{(i)}[\mathbf{R}_p,\mathbf{q}]a_i^+ a_i - \mathbf{m}_{0,12}[\mathbf{R}_p + 2a_e\tilde{\mathbf{m}}_{av}](a_1^+ a_2 + a_2^+ a_1) + H_v \tag{11}$$

Here $\tilde{\mathbf{m}}_{av} = (\tilde{\mathbf{m}}_{01} + \tilde{\mathbf{m}}_{02})/2$, and a_e is the linear response coefficient of the electronic polarization of the solvent (see section 2.4). The diagonal energies depend linearly on the nuclear reaction field of the solvent through the interaction with the solute dipole and quadratically through the energy of solute self-polarization

$$E_{0s}^{(i)}[\mathbf{R}_p,\mathbf{q}] = E_i + E_i^{disp} + F_i^{ind} - \tilde{\mathbf{m}}_{0i}\cdot\mathbf{R}_p - \frac{1}{2}\mathbf{R}_p\cdot\tilde{\alpha}_{0i}\cdot\mathbf{R}_p - \sum_n \gamma_{in}q_n \tag{12}$$

Here "0s" refers to the solute ("0") interacting with the solvent ("s")

$$\tilde{\mathbf{m}}_{0i} = \mathbf{f}_{ei}\cdot\mathbf{m}_{0i}, \qquad \tilde{\alpha}_{0i} = \mathbf{f}_{ei}\cdot\bar{\alpha}_{0i} \tag{13}$$

and

$$\mathbf{f}_{ei} = [\mathbf{1} - 2a_e\bar{\alpha}_{0i}]^{-1} \tag{14}$$

is the enhancement factor of the solute polarizability and the dipole moment due to the field created by the solvent electronic polarization.[29,39] The diagonal energy $E_{0s}^{(i)}$ in eq 12 includes the solvation energy due to the dispersive solute−solvent interactions E_i^{disp} and the free energy of solvation by induction forces

$$F_i^{ind} = -a_e\mathbf{m}_{0i}\cdot\mathbf{f}_{ei}\cdot\mathbf{m}_{0i} \tag{15}$$

Diagonalization of the two-state matrix in eq 11 leads[5] to the lower, $E_-[\mathbf{R}_p,\mathbf{q}]$, and upper, $E_+[\mathbf{R}_p,\mathbf{q}]$, adiabatic free energy surfaces depending on the nuclear reaction field $\mathbf{R}_p$ and the vibrational intramolecular modes **q**

$$E^{\pm}[\mathbf{R}_p,\mathbf{q}] = \frac{1}{2}(E_{0s}^{(1)}[\mathbf{R}_p,\mathbf{q}] + E_{0s}^{(2)}[\mathbf{R}_p,\mathbf{q}]) \pm \frac{1}{2}\Delta E[\mathbf{R}_p,\mathbf{q}] + H_v \tag{16}$$

where

$$\Delta E[\mathbf{R}_p,\mathbf{q}] = \sqrt{(\Delta E_{0s}[\mathbf{R}_p,\mathbf{q}])^2 + 4(V_{12}[\mathbf{R}_p])^2} \tag{17}$$

In eq 17, $\Delta E_{0s} = E_{0s}^{(2)}[\mathbf{R}_p,\mathbf{q}] - E_{0s}^{(1)}[\mathbf{R}_p,\mathbf{q}]$ and

$$V_{12}[\mathbf{R}_p] = \mathbf{m}_{0,12}\cdot\mathbf{R}_p + 2a_e\mathbf{m}_{0,12}\tilde{\mathbf{m}}_{av} \tag{18}$$

Equations 16−18 are the major result of our treatment. They establish the adiabatic free energy surfaces of a dipolar optical chromophore as a function of the nuclear configuration of the system and thus can be directly used to construct optical FC factors.

2.2. Vibronic Hamiltonian. The upper and lower free energy surfaces, depending on the system nuclear coordinates $\mathbf{R}_p$ and **q**, are the starting point for building the absorption and emission band shapes. The function $\Delta E[\mathbf{R}_p,\mathbf{q}]$ is strongly nonlinear in $\mathbf{R}_p$ and **q**, which makes it especially difficult to construct the vibrational envelope. To make the problem tractable, we linearize $\Delta E[\mathbf{R}_p,\mathbf{q}]$ in **q**

$$\Delta E[\mathbf{R}_p,\mathbf{q}] \simeq \Delta E[\mathbf{R}_p,\mathbf{q}_0^{\pm}] + \left.\frac{\partial\Delta E[\mathbf{R}_p,\mathbf{q}]}{\partial\mathbf{q}}\right|_{\mathbf{q}_0^{\pm}}\cdot(\mathbf{q} - \mathbf{q}_0^{\pm}) \tag{19}$$

around the equilibrium coordinate $\mathbf{q}_0^{\pm}$ defined through the relation

$$\partial E^{\pm}[\mathbf{R}_p,\mathbf{q}]/\partial\mathbf{q}|_{\mathbf{q}_0^{\pm}} = 0 \tag{20}$$

The **q**-derivatives in eqs 19 and 20 can be expressed through the difference in electron occupation numbers of the upper and lower surfaces at the same nuclear configuration of the system ("vertical" occupation difference)[6]

$$\Delta n[\mathbf{R}_p,\mathbf{q}] = n^-[\mathbf{R}_p,\mathbf{q}] - n^+[\mathbf{R}_p,\mathbf{q}] \tag{21}$$

with (see eqs 16 and 17)

$$n^\pm[\mathbf{R}_p,\mathbf{q}] = \frac{1}{2} \mp \frac{\Delta E_{0s}[\mathbf{R}_p,\mathbf{q}]}{2\Delta E[\mathbf{R}_p,\mathbf{q}]} \tag{22}$$

One then obtains for the **q**-derivative of the free energy gap

$$\left.\frac{\partial \Delta E[\mathbf{R}_p,\mathbf{q}]}{\partial \mathbf{q}}\right|_{\mathbf{q}_0^\pm} = -\Delta n^\pm[\mathbf{R}_p]\Delta\gamma_n \tag{23}$$

where

$$\Delta n^\pm[\mathbf{R}_p] = \Delta n[\mathbf{R}_p,\mathbf{q}_0^\pm] \tag{24}$$

The equilibrium coordinates of the nuclear normal modes are different for the upper and lower adiabatic surfaces. This is reflected by "+" and "−" superscripts in $\mathbf{q}_0^\pm$. Because of this, the difference in vertical occupation numbers (eq 24) at an equilibrium nuclear configuration is also state-dependent, which is reflected by the corresponding "±" superscript. From eq 20, $\mathbf{q}_0^\pm$'s are given by the self-consistent equation

$$q_{0n}^\pm = \kappa_n^{-1}[\gamma_n^{av} \pm (\Delta n^\pm/2)\Delta\gamma_n] \tag{25}$$

where $\gamma_n^{av} = (\gamma_{1n} + \gamma_{2n})/2$, $\Delta\gamma_n = \gamma_{2n} - \gamma_{1n}$, and for brevity, we will suppress the dependence of $\Delta n^\pm$ on $\mathbf{R}_p$ in the remainder.

Equation 25 indicates two important features characteristic of vibronic spectra in delocalized systems. First, equilibrium positions of normal vibrational modes shift with the change in electronic populations induced by the solvent. The vibrational Hamiltonian

$$H_v^\pm = \sum_n \left[\frac{\kappa_n}{2}(q_n - q_{0n}^\pm)^2 + T(q_n)\right] \tag{26}$$

couples the vibrational (**q**) and solvent ($\mathbf{R}_p$) nuclear modes through $\Delta n^\pm$ (eqs 24 and 25). Second, the force constants of the normal modes (second derivative of $E_\pm$ in **q**) also change with $\Delta n^\pm$.[17] Here, we will neglect the second-order effect of force constant modulation. To minimize the impact of the first-order expansion on our calculations, we will consider the alteration of the band shape relative to the spectrum in a nonpolar reference solvent. Following Reynolds et al.,[31] 2-methylbutane is considered as a reference below.

In the linearized form, the energy surfaces for intramolecular vibrations are harmonic with the equilibrium coordinates given by eq 25. Substitution of eqs 19, 23, and 25 into eqs 16−17 yields the upper and lower free energy surfaces in a form convenient for modeling the solvent-related changes in the spectral band relative to a reference band shape (the constant term, independent of $\mathbf{R}_p$, is omitted)

$$E^\pm[\mathbf{R}_p] = H_v^\pm[\mathbf{R}_p] - \tilde{\mathbf{m}}_{av}\cdot\mathbf{R}_p - \frac{1}{2}\mathbf{R}_p\cdot\tilde{\alpha}_{av}\cdot\mathbf{R}_p \pm \frac{1}{2}\Delta E^\pm[\mathbf{R}_p] \tag{27}$$

where $\tilde{\alpha}_{av} = (\tilde{\alpha}_{01} + \tilde{\alpha}_{02})/2$ and $H_v^\pm[\mathbf{R}_p]$ (eq 26) depends on the field $\mathbf{R}_p$ via eq 25. The energy gap between the upper and lower surfaces now depends on only one nuclear mode, the solvent nuclear reaction field

$$\Delta E^\pm[\mathbf{R}_p] = [(\Delta E_{0s}^\pm[\mathbf{R}_p])^2 + 4(V_{12}[\mathbf{R}_p])^2]^{1/2} \tag{28}$$

Here[41]

$$\Delta E_{0s}^\pm[\mathbf{R}_p] = \bar{\nu}_m^{ref} \mp \Delta\tau^\pm\lambda_v^{ref} + \delta F^{ind} - \Delta\tilde{\mathbf{m}}_0\cdot\mathbf{R}_p - \frac{1}{2}\mathbf{R}_p\cdot\Delta\tilde{\alpha}_0\cdot\mathbf{R}_p \tag{29}$$

is the diagonal energy difference shifted by the solvent relative to the mean of absorption and emission first spectral moments in the reference solvent

$$\bar{\nu}_m^{ref} = (\bar{\nu}_{abs}^{ref} + \bar{\nu}_{em}^{ref})/2 = \Delta E_{00} + \Delta E_{ref}^{disp} + \Delta F_{ref}^{ind} \tag{30}$$

where

$$\Delta E_{00} = E_2 - E_1 - \sum_n ({}^1/_2\kappa_n)(\gamma_{2n}{}^2 - \gamma_{1n}{}^2) \tag{31}$$

is the gas-phase 0−0 transition energy. In eq 29, $\Delta\tilde{\mathbf{m}}_0 = \tilde{\mathbf{m}}_{02} - \tilde{\mathbf{m}}_{01}$, $\Delta\tilde{\alpha}_0 = \tilde{\alpha}_{02} - \tilde{\alpha}_{01}$, and δF^{ind} is the change in induction stabilization relative to that in the reference solvent.

Equation 29 indicates that the effect of the solvent-induced mixing of the electronic states on the instantaneous energy gap is due to the line shift $\mp\Delta\tau^\pm\lambda_v^{ref}$ with the delocalization factor[43]

$$\Delta\tau^\pm = \frac{\Delta n^\pm}{\Delta n_{ref}^\pm} \tag{32}$$

and the vibrational reorganization energy in the reference solvent, $\lambda_v^{ref} = \Delta n_{ref}^\pm\lambda_v$, where

$$\lambda_v = \sum_n \Delta\gamma_n{}^2/2\kappa_n \tag{33}$$

is the gas-phase vibrational reorganization energy, measured as one-half of the gas-phase vibrational Stokes shift. Changes in the occupation number difference may result in asymmetry between the absorption and emission vibrational envelopes even in a nonpolar reference solvent. This effect, combined with a possible alteration in effective vibrational force constants, leads to a redistribution of intensities between the normal modes. This distortion of the gas-phase band shape is indeed seen for C153 when the chromophore is transferred from the gas phase to 2-methylbutane.[40] In the present modeling, this effect is taken into account by adopting the experimental reference band shapes. For the band shift induced in polar solvents in eq 29, we will neglect the difference in absorption and emission reorganization energies in the reference solvent and consider λ_v^{ref} to be equal to one-half of the Stokes shift.

The delocalization parameter in eq 32 is given by the self-consistent relation

$$\Delta\tau^\pm = \frac{\Delta E_{0s}^\pm[\mathbf{R}_p]\Delta E^\pm[0]}{\Delta E_{0s}^\pm[0]\Delta E^\pm[\mathbf{R}_p]} \tag{34}$$

Because of the large energy gap for the optical excitation of C153 in the inverted CT region, $\Delta\tau^\pm$ is very close to unity. The variation in $\Delta\tau^\pm$ depends on the solvent field and does not exceed −0.1 in the present calculations.

2.3. Optical Line-Shape. The dependence of the overall transition intensity ($I_{abs/em}(\bar{\nu})$, where $\bar{\nu}$ is the wavenumber of the incident light, cm^{-1}) on system nuclear coordinates arises both from transition moment, which results in additional powers of the frequency $\bar{\nu}$[42] and the so-called density-of-states weighted FC factor, FCWD.[1] The normalized FCWD can be expressed as

$$\mathrm{FCWD}_{abs/em}(\bar{\nu}) = \sum_{\mathbf{m},\mathbf{k}} \langle |\langle \chi_{+\mathbf{k}} | \chi_{-\mathbf{m}} \rangle|^2 \delta(\Delta E^{\pm}[\mathbf{R}_p] + \epsilon_{\mathbf{k}} - \epsilon_{\mathbf{m}} - \bar{\nu}) \rangle_{\mp,v} \quad (35)$$

where

$$\epsilon_{\mathbf{k}} - \epsilon_{\mathbf{m}} = \sum_n \bar{\nu}_n k_n - \sum_n \bar{\nu}_n m_n \quad (36)$$

and $\bar{\nu}_n$ are vibrational frequencies of the normal modes defined by the vibrational Hamiltonian in eq 26; $\chi_{\pm\mathbf{k}}$ are the vibrational wave functions.[14] **m** and **k** denote *n*-component vectors of vibrational quantum numbers in the initial and final state for each normal vibrational mode. The statistical average $\langle ... \rangle_{\mp,v}$ is taken over the vibrational excitations in the initial state ("v") and the statistical distribution of the solvent nuclear reaction field with

$$\langle ... \rangle_{\mp} = (Q^{\mp})^{-1} \int ... e^{-\beta E^{\mp}[\mathbf{R}_p]} P[\mathbf{R}_p]\, d\mathbf{R}_p \quad (37)$$

and

$$Q^{\mp} = \int e^{-\beta E^{\mp}[\mathbf{R}_p]} P[\mathbf{R}_p]\, d\mathbf{R}_p \quad (38)$$

Here, $P[\mathbf{R}_p]$ is the probability of creating a nonequilibrium nuclear reaction field $\mathbf{R}_p$ in the solvent surrounding the chromophore.

The transition from a reference, nonpolar solvent to a polar solvent shifts the equilibrium coordinate of each normal mode, $q_{0n}^{\pm} = \gamma_n^{av}/\kappa_n \pm \Delta\gamma_n^{ref}\Delta\tau^{\pm}/2\kappa_n$. This shift can be accounted for by a rescaling of the difference electron−phonon coupling, $\Delta\gamma_n^{ref} \rightarrow \Delta\gamma_n^{ref}\Delta\tau^{\pm}$, which also implies a rescaling of the vibrational reorganization energy

$$\lambda_v^{\pm} = (\Delta\tau^{\pm})^2 \lambda_v^{ref} \quad (39)$$

Since quantum vibrational envelope is non-Gaussian, explicit knowledge of the whole set $\{\gamma_n, \bar{\nu}_n\}$ is necessary for a complete description of the solvent-induced alteration of the vibrational envelope. An approximate solution is available by rescaling spectra measured in the reference solvent.

In the harmonic approximation, the normalized spectral distribution of absorption ("−") and emission ("+") in the reference solvent is[1b]

$$\mathrm{FCWD}_{abs/em}^{ref}(\bar{\nu}_{abs/em}^{ref} + \bar{\nu}) = \int_{-\infty}^{\infty} (dx/2\pi) e^{-ix\lambda_v \mp i\bar{\nu}x} \prod_n e^{C_n^2 f_n(\bar{\nu}_n x)} \quad (40)$$

where $C_n^2 = \Delta\gamma_n^{ref}/2\kappa_n\bar{\nu}_n$, $f_n(x) = i\sin(x) - (2\bar{n}_n + 1)(1 - \cos(x))$ and $\bar{n}_n$ is the average quantum number of *n*th vibrational mode. The scaled spectrum

$$(\Delta\tau^{\mp})^{-1}\mathrm{FCWD}_{abs/em}^{ref}(\bar{\nu}_{abs/em}^{ref} + \bar{\nu}/\Delta\tau^{\mp}) = \int_{-\infty}^{\infty} (dx/2\pi) e^{-ix\Delta\tau^{\mp}\lambda_v \mp i\bar{\nu}x} \prod_n e^{C_n^2 f(\Delta\tau^{\mp}\bar{\nu}_n x)} \quad (41)$$

then correctly reproduces polarity changes of the second vibrational spectral moment for each normal mode but does not give correct higher moments. The linear with $\Delta\tau^{\pm}$ shift of the first spectral moment is included in the energy gap in eq 29. Equation 41 allows us to define the vibrational spectrum in a polar solvent by simple scaling of the spectrum in the reference solvent. Note that this approximation does not assume a Gaussian form of the vibrational envelope. Each normal mode is characterized by its own intensity, and the total spectrum can be asymmetric. The vibrational spectrum in a polar solvent is then given by the relation

$$\sum_{\mathbf{m},\mathbf{k}} \langle |\langle \chi_{+\mathbf{n}} | \chi_{-\mathbf{m}} \rangle|^2 \delta(\epsilon_{+\mathbf{k}} - \epsilon_{-\mathbf{m}} - x) \rangle_v = (1/\Delta\tau^{\mp})\mathrm{FCWD}_{abs/em}^{ref}(\bar{\nu}_{abs/em}^{ref} + x/\Delta\tau^{\mp}) \quad (42)$$

The FC factor in eq 35 is then given by the convolution

$$\mathrm{FCWD}_{abs/em}(\bar{\nu}) = \int_{-\infty}^{\infty} dx \langle (\Delta\tau^{\mp})^{-1} \delta(\bar{\nu} - x - \Delta E^{\mp}[\mathbf{R}_p]) \mathrm{FCWD}_{abs/em}^{ref}(\bar{\nu}_{abs/em}^{ref} + x/\Delta\tau^{\mp}) \rangle_{\mp} \quad (43)$$

Note that this convolution cannot be reduced to an integral over the separate solvent-induced and vibrational envelopes because the factor $\Delta\tau^{\mp}$ depends on the nuclear reaction field $\mathbf{R}_p$.

Equations 27−43 establish a general solution for the solvent-induced spectral band shape at arbitrary orientations of the dipole moments $\mathbf{m}_{0i}$ and $\mathbf{m}_{0,12}$ and an anisotropic second-rank polarizability tensor α_{0i} of the chromophore. The reaction field $\mathbf{R}_p$ serves as a three-dimensional reaction coordinate of the solvent nuclear fluctuations driving CT. In fact, one does not need to include all three components of the reaction field. For general orientations of the difference and transition dipoles, it is sufficient to consider only two components of $\mathbf{R}_p$ in the plane formed by $\Delta\tilde{\mathbf{m}}_0$ and $\mathbf{m}_{0,12}$: the longitudinal component $R_{||}$ parallel to $\Delta\tilde{\mathbf{m}}_0$ and the transverse component $R_{\perp}$ perpendicular to $\Delta\tilde{\mathbf{m}}_0$. This assumption, however, is possible if the polarizability tensor of the chromophore is diagonal in the $\{R_{||}, R_{\perp}\}$ coordinates and the two polarizability components in the plane formed by rotations around $R_{||}$ are equal to each other. As insufficient information about polarizability anisotropy of C153 is currently available, we will assume an isotropic polarizability $\alpha_{0i}^{\alpha\beta} = \delta_{\alpha\beta}\alpha_{0i}$ throughout the remainder of the paper.[44]

By applying the property of the δ-function

$$\int_{-\infty}^{\infty} \delta(x - f(x)) g(x)\, dx = g(x_0)|f'(x)|^{-1}|_{x_0 = f(x_0)} \quad (44)$$

one can eliminates the integral over $R_{||}$ in eq 43, yielding

$$\mathrm{FCWD}_{abs/em}(\bar{\nu}) = \frac{2\pi}{Q^{\mp}} \sum_k \int_0^{\infty} dR_{\perp}\, R_{\perp} \times \int_{-\infty}^{\infty} \frac{dx}{\Delta\tau^{\mp}} \mathrm{FCWD}_{abs/em}^{ref}(\bar{\nu}_{abs/em}^{ref} + x/\Delta\tau^{\mp}) \times [\Delta E'_{\mp}(R_{\perp}, R_{||}^{(k)}(R_{\perp}))]^{-1} P[R_{\perp}, R_{||}^{(k)}(R_{\perp})] \times \exp(-\beta E^{\mp}[R_{\perp}, R_{||}^{(k)}(R_{\perp})]) \quad (45)$$

Here, $R_{||}^{(k)}(R_{\perp})$'s are the solutions of the equation

$$\Delta E^{\mp}[R_{||}, R_{\perp}] = \bar{\nu} - x \quad (46)$$

TABLE 1: Solvent Properties ($T = 293$ K)[31,45] [a]

solvent	m, D	q, D × Å	σ, Å	η[c]	α, Å^3	solvent Stokes shift[b] $\Delta\bar{\nu}^s_{st}$	dip.	quad.
2-methylbutane (2-mb)	0.0	0.50[d]	5.60	0.477	10.1	0.0	0.0	0.0
toluene (tol)	0.38	7.92	5.66	0.534	12.3	0.50	0.11	0.39
benzene (ϕh)	0.0	8.35	5.27	0.515	10.4	0.59	0.0	0.59
p-xylene (*p*-xy)	0.02	7.69	6.00	0.550	14.2	0.37	0.06	0.31
chloroform (chl)	1.04	2.85	5.05	0.503	8.5	0.58	0.51	0.07
dichloromethane (dcm)	1.14	4.41	4.62	0.482	6.5	0.94	0.79	0.15
tetrahydrofuran (thf)	1.75	5.39	5.10	0.511	7.9	1.23	1.11	0.12
methyl acetate (mea)	1.76	10.41	5.77	0.524	10.5	1.23	0.87	0.36
acetone (acet)	2.85	4.71	4.78	0.464	6.3	1.69	1.64	0.05
nitromethane (nme)	3.57	5.42	4.36	0.483	5.0	1.94	1.90	0.04
dimethyl sulfoxide (dmso)	3.96	9.17	4.96	0.540	8.0	1.96	1.88	0.08
acetonitrile (acn)	3.90	2.49	4.14	0.424	4.5	1.89	1.87	0.02

[a] Solvents are listed in the order of increasing experimental Stokes shift.[31] [b] Calculated (APM) solvent-induced Stokes shift ($\Delta\bar{\nu}^s_{st}$) and its partitioning into dipolar ("Dip.") and quadrupolar ("Quad.") solvation components. [c] $\eta = (\pi/6)\rho\sigma^3$ is the packing density of the solvent. [d] Calculated in the present study.

that give roots depending on the transverse field component, and

$$\Delta E'_{\mp}(R_\perp, R_{||}^{(k)}(R_\perp)) = \left.\frac{\partial \Delta E^{\mp}[\mathbf{R}_p]}{\partial R_{||}}\right|_{R_{||}=R_{||}^{(k)}} \tag{47}$$

Equation 46 is formally a fourth-order polynomial in $R_{||}$. It contains, however, a complex dependence on $\mathbf{R}_p$ through $\Delta\tau^{\pm}$. The numerical solutions $R_{||}^{(k)}(R_\perp)$ are then searched as roots of the fourth-order polynomial in $R_{||}$ within an iteration procedure that includes a self-consistent calculation of $\Delta\tau^{\pm}$ as given by eq 34.

2.4. Solvent Response. Equation 45 gives a general recipe for calculating the optical band shape in liquid solutions for a general form of the solvent response given by the distribution function $P[\mathbf{R}_p]$. For an explicit calculation of the optical lineshape, one should take two steps further: (i) define a specific form for the distribution function $P[\mathbf{R}_p]$ and (ii) formulate an explicit solvent model relating the solvent response to parameters of a particular liquid used as a solvent. As the first step, we adopt here the LRA that gives $P[\mathbf{R}_p]$ in the form of a Gaussian function

$$P[\mathbf{R}_p] = \exp[-\beta \mathbf{R}_p^2/4a_p] \tag{48}$$

The linear response coefficient a_p defines the strength of nuclear solvation. It relates the chemical potential of solvation by the solvent nuclear degrees of freedom to the squared solute dipole (see eq 51 below). Parameter a_p is a major factor in defining nuclear reorganization effects on optical transitions. Apart from a_p, the solvent-induced band shape is affected by the response coefficient a_e, corresponding to the linear response by the electronic solvent polarization. Their sum gives the total solvent response coefficient

$$a = a_e + a_p \tag{49}$$

For a dipolar solute, linear response implies that the solvation chemical potential is a quadratic function of the solute dipole moment. The solvation chemical potential due to electronic polarization is then

$$\mu_e = -a_e f_{ei} m_{0i}^2 \tag{50}$$

The nuclear polarization produces the solvation chemical potential

$$\mu_p = -a_p f_i f_{ei} m_{0i}^2 \tag{51}$$

where $f_i = [1 - 2a\bar{\alpha}_{0i}]^{-1}$ and the response coefficient a is given by eq 49.

The second step in defining the solvent response is to formulate an explicit solvent model to calculate the response coefficients a_e and a_p. We adopt here the representation of the solvent as a fluid of hard-sphere (HS) particles with diameter σ, permanent dipole m, quadrupole moment q, and isotropic polarizability α. The vacuum dipole moments,[45] quadrupole moments,[31] and dipolar polarizabilities[45] for the solvents used in the calculations are taken from the literature and are listed in Table 1. The HS diameters of the solvent molecules are empirically fitted to isothermal compressibilities of real solvents.[45] The choice of the solvents listed in Table 1 is limited by the requirement to have both the HS diameters[45] and quadrupole moments available.[31] The solute is represented by a HS of the radius R_0 with a centered dipole moment $\mathbf{m}_{0i}$ and the isotropic polarizability α_{0i}. The latter is split into the component due to the $1 \rightarrow 2$ electronic transition and the polarizability $\bar{\alpha}_{0i}$ due to virtual transitions to all other excited states (eq 10). The model does not include many specific features of real solvents but incorporates several physically important factors characteristic of molecular liquid solvents that are often omitted both in continuum models and in computer simulations of solvation. The continuum model does not account for density fluctuations of the solvent. Solvent, as well as solute, polarizability is often omitted from computer modeling of solvation. The present approach has already shown its ability to reproduce experimental entropies of reorganization, a quantity incorrectly accounted for by cavity models,[46] to give reasonable rate constant prefactors when used to analyze the temperature dependence of ET rates[47] and to generate spectroscopic parameters for optical ET in high-density[32] and low-density[48] dipolar and nondipolar solvents.

Another attractive feature of the polarizable dipolar−quadrupolar HS solvent model is that it permits an analytical solution for the linear response coefficient through the Padé-truncated formulation of perturbative liquid state theories.[49] The response functions can be separated into factors involving the effective solute radius (R_{eff}) and the solvent polarity (Padé approximant, P)

$$a = R_{eff}^{-3} P(m,q,\alpha), \qquad a_e = R_{eff}^{-3} P(0,0,\alpha) \tag{52}$$

The effective radius of a dipolar solute depends on the ratio of HS solute and solvent diameters (respectively, σ_0 and σ) and

TABLE 2: Parameters of C153 from Experiment and Calculations

	m_{01}, D	Δm_0, D	$m_{0,12}$, D	α_{01}, Å^3	$\Delta\alpha_0$, Å^3
experiment	6.6[a]	5.8−7.0[b] 4.9[d]	5.78[c] 5.70[e]		4−6[b]
present calculations					
INDO/s	7.4[f]	7.53[f]	6.11[f]	19.5[f]	13.5[f]
ab initio	6.14[g]	3.74[g]	6.03[g]	25.8[g]	4.4[g]
other semiempirical results	6.4−6.7[h]	7.0−7.3[h]	5.46[i]	20.0[j]	13.0[h]

[a] Ref 50a; dielectric measurements in chloroform solution. See: C. R. Moylan et al., *Chem. Mater.* **1993**, *5*, 1499. [b] Stark measurements in toluene and 2-Me thf.[28] [c] Gas-phase transition dipole from ref 40. [d] Refs 50d and 28 contain the most recent lists of Δm_0 from different sources. [e] Average from absorption spectra in 14 solvents, ref 50b. [f] Results obtained by the INDO/s method of Zerner et al[53] within the framework of single-excitation configuration interaction (CIS) based on the ground-state self-consistent (SCF) wave function. Polarizabilities were obtained using second-order perturbation theory. [g] Ab initio results using a 6-21G* basis and CIS wave functions (see footnote f).[54] Polarizabilities were based on exact linear response calculations within the CIS framework (for a chosen orbital basis). [h] AM1 calculations from ref 51. [i] AM1 calculations from ref 50b. [j] Semiempirical calculations from ref 40.

the reduced solvent density, $\rho\sigma^3$ (ρ is the solvent number density), through the radial solute−solvent pair distribution function $g_{0s}(r)$

$$R_{\text{eff}}^{-3} = 3\int_0^\infty \frac{dr}{r^4} g_{0s}(r) \qquad (53)$$

A polynomial fit of the numerical integral in eq 53 is given in ref 49 and is compared to the results of computer simulations in ref 49c. The Padé approximant $P(m,q,\alpha)$ of the dipolar−quadrupolar solvent response was derived in ref 28 and is given in Appendix A.

2.5. Parameters. Vacuum parameters of C153 taken from experimental literature[40,50] and calculations[51,52] are listed in Table 2. The present INDO/s[53] configuration interaction (CI) calculations, based on single excitations (CIS) from the self-consistent field (SCF) ground state, yield the dipole moments, $m_{01} = 7.4$ D and $\Delta m_0 = 7.6$ D, in reasonable agreement with available experimental data and results from other semiempirical calculations (Table 2). Ab initio[54] CIS calculations (6-21G* basis) yield a smaller Δm_0 value (3.9 D). The choice of the INDO/s dipole moments instead of the ab initio values in the present solvation calculations is supported by the solute radius fitting to experimental Stokes shift data (see below). When the ab initio Δm_0 is used in the fit, the maximum of the dependence of the Stokes shift on the solute HS radius ($R_0 = \sigma_0/2$) falls far below experimental values, and the fitting procedure does not yield a reasonable estimate for R_0. For the transition dipole, the experimental gas-phase magnitude, $m_{0,12} = 5.78$ D,[40] is adopted for the calculations (the calculated $m_{0,12}$ values in Table 2 are quite similar to the experimental value).

Ab initio values for $\alpha_{01} = 25.8$ Å^3 and $\Delta\alpha_0 = 4.4$ Å^3 are employed here. The choice of ab initio over INDO/s values for $\Delta\alpha_0$ is adopted since the INDO/s results are based on a sum-over-states perturbative result, whereas the ab initio calculations use essentially an exact treatment within linear response (for the given basis set). The ab initio $\Delta\alpha_0$ compares favorably with the Stark data,[28] and the ab initio α_{01} is close to the $\alpha_{01} = 28$ Å^3 obtained from the Miller's empirical method of additive hybrid atomic polarizabilities.[55]

In addition to the calculated and experimental gas-phase parameters, we use the experimental band-shape absorption and emission profiles $\text{FCWD}_{\text{abs/em}}^{\text{ref}}(\bar{\nu})$ in 2-methylbutane. The only solute parameter that remains undefined from the gas-phase measurements and quantum calculations is the effective HS radius of the chromophore, R_0. This radius was obtained as the best-fit value reproducing experimental Stokes shifts[31,56] (Table 3, second column). The resulting value $R_0 = 4.89$ Å coming out of the fit is somewhat higher than the value of 4.76 Å calculated by Rechthaler and Köhler on the basis of molecular dimensions of C153.[52] The quality of the fit is shown in Figure 2 (filled points). [The open points refer to the calculation that does not take into account the coupling of the solvent and intramolecular vibrational modes (see below).] Note that R_0 is the only fitting parameter of the model; the optical band-shape calculations are based on the vacuum properties of C153, experimental spectra in 2-methylbutane, and the radius R_0.

Fitting the solute radius is not a trivial problem in the case of polarizable/delocalized chromophores. The procedure is complicated by the fact that the Stokes shift as a function of the solute radius passes through a maximum in strongly polar solvents (Figure 3). This behavior is very different from the naive expectation of a trend $\propto \Delta m_0^2/R_0^3$, as in the case of localized systems. Two factors contribute to the more complicated dependence. The decrease of the radius leads to a stronger solvation power both directly through the effective radius R_{eff} in eq 53 and through the correction coefficient f. Electronic delocalization plays an opposite role. An increase of solvation power related to the decrease in R_0 enhances delocalization. As the degree of delocalization (defined in terms of the vacuum adiabatic basis) becomes appreciable, the Stokes shift starts to decrease and eventually dominates over the increase due to a stronger solvent response, yielding a maximum as a function of the solute radius. The existence of a broad maximum implies

TABLE 3: Experimental Stokes Shifts and Half-intensity Widths for C153 (10^3 cm^{-1})

	$\Delta\bar{\nu}_{\text{st}}^{\text{exp}}$		$\Gamma_{\text{abs}}^{\text{exp}}$		$\Gamma_{\text{em}}^{\text{exp}}$		
solvent	I[a]	II[b]	I	II	I	II	III[c]
toluene	4.62		3.67		3.35		
benzene	4.77		3.65		3.31		2.86
p-xylene	4.80		3.67		3.48		
chloroform	4.85		3.69		3.20		
dichloromethane	5.06		3.68		3.20	3.45	3.02
tetrahydrofuran	5.34	6.01	3.79	4.21	3.36		
methyl acetate	5.55		3.87		3.37		
acetone	5.72	6.26	3.83		3.30	3.43	3.06
nitromethane	5.73		3.89		3.18		
dimethyl sulfoxide	5.71	6.71	3.91	4.09	3.32		3.38
acetonitrile	6.03	6.45	3.89	4.06	3.27	3.42	3.07

[a] Ref 31. [b] Ref 57. [c] Ref 52.

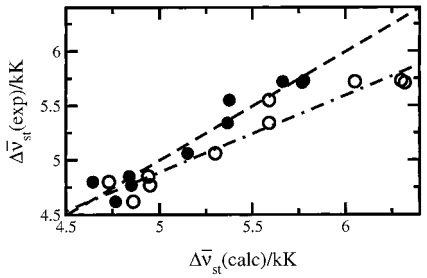

Figure 2. Experimental Stokes shift of C153[31] vs the calculated (APM, filled circles) Stokes shift for 10 solvents (2-methylbutane and acetonitrile excluded) listed in Table 3, based on $R_0 = 4.89$ Å. Open circles show the result of calculation excluding the vibrational−solvent coupling. The dashed and dash−dotted lines are linear regressions through the filled and open points, respectively. The regression slopes are 0.999 (dashed line) and 0.707 (dash−dotted line).

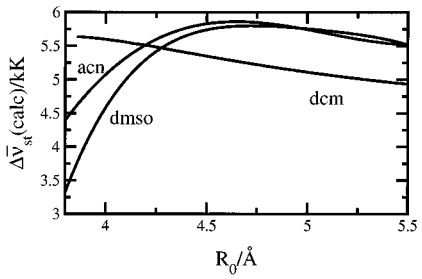

Figure 3. Calculated Stokes shift $\Delta\bar{\nu}_{st}^{s}$ vs the solute radius R_0 in acetonitrile (acn), dimethyl sulfoxide (dmso), and dichloromethane (dcm).

that there is a wide range of radii that result in essentially the same magnitude of the Stokes shift so that, in practical applications, one should exercise caution when fitting geometrical parameters to experimental data in strongly polar solvents. Weakly polar solvents may be more reliable in this sense, as they demonstrate only a monotonic decay of the Stokes shift with the solute radius (dcm in Figure 3).

3. Results

The theoretical derivation presented above shows that the inclusion of solvent-induced mixing of the vacuum adiabatic states leads to profound qualitative changes in the way the optical FCWD factor in condensed phases is calculated. Noteworthy is that partial CT couples the solvent and vibrational nuclear modes, making it impossible to use the convolution relation

$$\mathrm{FCWD}_{\mathrm{abs/em}}(\bar{\nu}) = \int_{-\infty}^{\infty} \mathrm{FCWD}^{\mathrm{s}}_{\mathrm{abs/ems}}(\bar{\nu} - x)\mathrm{FCWD}^{\mathrm{ref}}_{\mathrm{abs/em}}(x)\,\mathrm{d}x \tag{54}$$

mixing the solvent-induced spectral profile $\mathrm{FCWD}_{\mathrm{abs/ems}}(\bar{\nu})$ with the reference vibrational envelope $\mathrm{FCWD}^{\mathrm{ref}}_{\mathrm{abs/em}}(\bar{\nu})$ measured in the gas phase or in a reference nonpolar solvent. It is instructive, however, to understand the effects of electron delocalization on the solvent-induced and vibrational profiles separately. We will therefore start with considering the solvent-induced FC envelope

$$\mathrm{FCWD}^{\mathrm{s}}_{\mathrm{abs/em}}(\bar{\nu}) = \langle \delta(\Delta E^{\mp}[\mathbf{R}_{\mathrm{p}}] - \bar{\nu})\rangle_{\mp} \tag{55}$$

assuming no vibrational modes coupled to the transferred electron ($\gamma_{in} = 0$).

3.1. Solvent-Induced Band. The solvent effect on the transition between the states 1 and 2 considered in the present model includes three components: (i) solvation of the fixed charges (dipole moments) of the chromophore, (ii) self-polarization of the solute's electronic cloud due to polarizability, and (iii) change in the electronic occupation numbers induced by the off-diagonal coupling of the transition dipole to the solvent field. Here we consider the consequences of these factors for the line position and width.

The average over the nuclear reaction field in eq 55 reduces to integrals over the longitudinal and transverse components of the field. The δ-function in eq 55 eliminates the integral over the longitudinal field (eq 44). The solvent-induced line is then given in terms of a one-dimensional integral over the transverse reaction field (similarly to that in eq 45) that can be taken analytically in two limiting cases: (i) zero transition dipole (DPM, $m_{0,12} = 0$)[29] and (ii) the TSM ($\bar{\alpha}_{0i} = 0$) (Appendix B).[5] In the case of the C153 dye, both factors, the polarizability $\bar{\alpha}_{0i}$ and the transition dipole $m_{0,12}$, considerably affect the spectra,

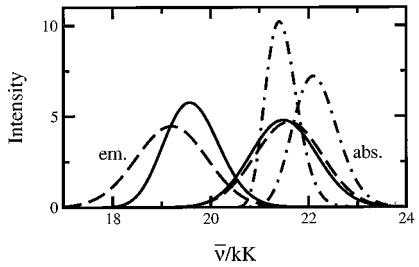

Figure 4. Absorption (abs.) and emission (em.) solvent-induced lineshapes of C153 in acetonitrile calculated according to the present model (APM, solid lines), neglecting electronic delocalization (DPM, dashed lines),[29] and in the two-state model (TSM, dash−dotted lines).[5] Solute and solvent parameters are from Tables 1 and 2 with $R_0 = 4.89$ Å.

TABLE 4: Spectral Parameters of the Solvent-Induced Band Shapes (10^3 cm^{-1}) Calculated in the Present Adiabatic Polarizable Model (APM), the Two-State Model (TSM), and the Diabatic Polarizable Model (DPM)

	APM			TSM			DPM		
solvent	$\Delta\bar{\nu}_{st}^{s}$	$\sigma_{abs}{}^{a}$	$\sigma_{em}{}^{a}$	$\Delta\bar{\nu}_{st}^{s}$	$\sigma_{abs}{}^{a}$	$\sigma_{em}{}^{a}$	$\Delta\bar{\nu}_{st}^{s}$	$\sigma_{abs}{}^{a}$	$\sigma_{em}{}^{a}$
toluene	0.50	0.45	0.46	0.28	0.30	0.26	0.46	0.46	0.46
benzene	0.59	0.55	0.56	0.33	0.35	0.30	0.57	0.56	0.57
p-xylene	0.37	0.31	0.31	0.21	0.22	0.20	0.32	0.31	0.32
chloroform	0.58	0.54	0.54	0.33	0.35	0.30	0.55	0.54	0.55
dichloromethane	0.94	0.94	0.92	0.48	0.54	0.41	0.98	0.96	0.99
tetrahydrofuran	1.23	1.27	1.17	0.58	0.69	0.48	1.33	1.28	1.35
methyl acetate	1.23	1.26	1.17	0.60	0.70	0.49	1.33	1.28	1.36
acetone	1.69	1.85	1.49	0.68	0.87	0.50	1.98	1.88	2.04
nitromethane	1.94	2.29	1.50	0.68	0.91	0.47	2.51	2.36	2.61
dimethyl sulfoxide	1.96	2.32	1.48	0.65	0.88	0.44	2.58	2.43	2.69
acetonitrile	1.89	2.16	1.51	0.69	0.92	0.49	2.37	2.23	2.47

[a] Calculated according to eq 5.

thus requiring consideration at the more general APM level developed in the present study. Figure 4 compares the solvent-induced absorption and emission profiles (eq 55) generated in the TSM, DPM, and APM approximations. Solid lines indicate the APM model (eq 55), the dashed lines refer to the DPM ($m_{0,12} = 0$, eq B1), and the dash−dotted lines correspond to the TSM ($\bar{\alpha}_{0i} = 0$, eq B5). The emission line is broader than the absorption line due to a higher excited-state polarizability when electron delocalization is neglected (DPM). The inclusion of electronic delocalization through the transition dipole (APM) narrows the emission line and reduces the maxima separation. Finally, the neglect of polarizability from higher lying electronic states in the TSM generates an even narrower emission band. The line shape is therefore a result of a compensation between the polarizability effect tending to increase both the emission width and the Stokes shift for $\Delta\alpha_0 > 0$ and the opposite effect of electronic delocalization. The results for the solvent-induced Stokes shifts and width in different solvents calculated using the TSM, DPM, and APM are summarized in Table 4.

Solvent-induced Stokes shifts were calculated as the difference between first spectral moments for absorption and emission. Splitting of the calculated Stokes shift into the dipolar and quadrupolar components (Appendix A) is given in Table 1, which lists also the dipole and quadrupole moments of the solvents used in the analysis. The quadrupolar solvation effect is negligible (on a relative basis) for strongly polar solvents like acetonitrile and nitromethane but is the major solvation component for nondipolar or very weakly nondipolar solvents (toluene, benzene, *p*-xylene). The general outcome of this analysis is that, except for some solvents with very high quadrupole moment (methyl acetate), quadrupolar solvation makes a very moderate impact on the Stokes shift in polar

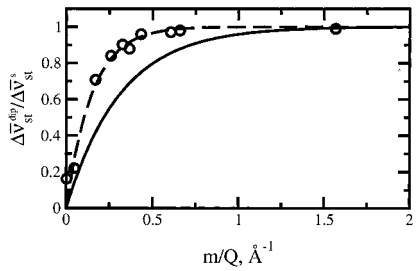

Figure 5. Fraction of the dipolar component in the solvent-induced Stokes shift from data listed in Table 1 (points). The regression lines correspond to the fit $1 - \exp(-pm/Q)$, with $p = 6.8$ for the present data (dashed line) and $p = 3.2$ for the analysis by Reynolds et al.[31]

solvents (Figure 5). This is a significant result, indicating that even for weakly polar solvents (chloroform), one can rely on dipolar solvent models, as had been done for many years[1a] and was recently put into question[31] (see Discussion).

The solid line in Figure 5 shows the result of splitting the solvent-induced Stokes shift into dipolar and quadrupolar components performed by Reynolds et al.[31] As is seen, their analysis, based on computer simulations of one solvent molecule interacting with C153, gives a wider range of m/Q ratios for which quadrupolar solvation is significant. Especially for dipolar solvents with large quadrupole moments, the many-body dipole−quadrupole coupling between the solvent molecules significantly affects the solvation energetics,[35] and full-size simulations may be necessary to include such effects. Note that the inclusion of the solute quadrupole additionally to the dipole moment considered here is expected to enhance the relative contribution of the dipolar solvent component in the Stokes shift, thus making the function in Figure 5 to rise even more steeply. This is because the dipole−quadrupole interactions are stronger and more long-ranged than the quadrupole−quadrupole interaction, resulting in a stronger coupling of the solute quadrupole to solvent dipoles than to solvent quadrupoles.

The solvent dependence of the Stokes shift and the line position when $m_{0,12} \neq 0$ shows only quantitative differences compared to the traditional results corresponding to $m_{0,12} = 0$. The solvent dependence of the spectral width is, on the contrary, qualitatively different from standard expectations. Our calculated solvent-induced spectral widths (APM, TSM, and DPM) for 11 solvents are listed in Table 4. The main qualitative result is that the solvent-induced absorption width approximately follows the relation

$$\beta\sigma_s^2 = 2\lambda_s \qquad (56)$$

where the subscript "s" stands for the solvent component. The APM emission width deviates dramatically from this relation, passing through a maximum as a function of solvent polarity (Table 4, fourth column; Figure 6). The TSM qualitatively reproduces this result but gives values too low for both the Stokes shifts and the widths. The APM formalism, combining features of both the TSM and DPM approximations, provides a reasonable description of spectral profiles. This comparison allows us to conclude that transitions to higher excited states and solvent-induced mixing of adiabatic states are both crucial for reproducing the optical band shape.

Equation 56 is a consequence of using the LRA, in conjunction with the separation of the electronic and nuclear time scales and the assumption of state-independent polarizability. Another consequence of these assumptions is the linear relation between the absorption/emission width and the solvent-induced shift[22]

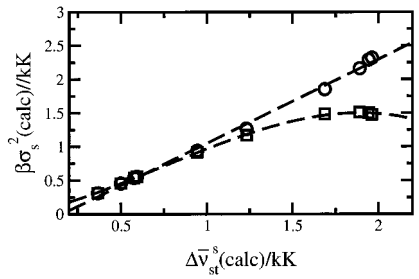

Figure 6. Calculated (APM) solvent component of the width vs the solvent-induced Stokes shift for absorption (circles) and emission (squares). Points indicate 11 solvents from Table 1 (2-methylbutane excluded). The dashed lines are regressions through the points.

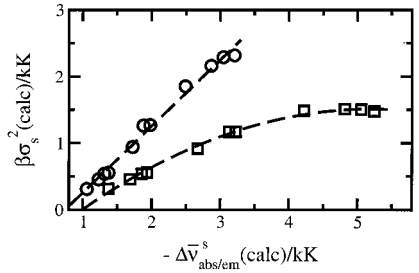

Figure 7. Calculated (APM) solvent-induced spectral width (eq 5) vs the solvent-induced shift (relative to the gas-phase spectrum) of absorption (circles) and emission (squares) lines. Points indicate the solvents listed in Table 1 (2-methylbutane excluded), and dashed lines are regressions through the points.

$$-\Delta\bar{\nu}_{abs/em}^{s} = \beta\sigma_{abs/em}^2 \frac{m_{01/2}}{\Delta m_0} + (m_{02}^2 - m_{01}^2)a_e \qquad (57)$$

where $m_{01/2}$ is equal to m_{01} for absorption and m_{02} for emission. Figure 7 shows the dependence of the APM widths on the APM solvent-induced shifts for absorption and emission (relative to the gas-phase transition). The dependence of $\beta\sigma_{abs}^2$ on $\Delta\bar{\nu}_{abs}^{s}$ is close to a linear one. The trend deviates considerably from a linear one for emission. This is the reason for the curved dependence of $\beta\sigma_{em}^2$ on $\Delta\bar{\nu}_{st}$ seen in Figure 6.

3.2. Solvent−Vibrational Band. The total Stokes shift and spectral widths are the results of the combined effects of the shifts and inhomogeneous broadenings due to solvent and vibrational nuclear modes. These are calculated from eq 45 and compared to experiment in Figures 8−10 and Table 5. The experimental Stokes shifts are prone to considerable uncertainties, as first spectral moments are noticeably affected by the choice of the frequency range used for integration. For instance, Gustavsson et al.[57] have reported higher Stokes shifts than those given by Reynolds et al.[31] (respectively, the columns labeled II and I in Table 3). Along with the higher absolute values, there are also qualitative differences: dimethyl sulfoxide (dmso) appears to be a more polar solvent than acetonitrile according to Gustavsson et al.,[57] in contrast to the data from Reynolds et al.[31] We used the latter data for the theory-experiment comparison, as they provide the most comprehensive list of spectral data in various solvents compared to other literature data. They are seen to agree generally well with our calculations.

The most puzzling feature of the solvent progression of the spectral widths of C153, as is seen from the results of Reynolds et al. (Figure 1),[31] is the opposite signs of the slopes of $\beta\sigma_{abs}^2$ and $\beta\sigma_{em}^2$ versus the Stokes shift. Comparison of the data from Reynolds et al.[31] used in Figure 1 to other literature data (Table 3) does not offer clear support for an unambiguous decay of the emission width with solvent polarity. A conservative analysis of the data from Reynolds et al.,[31] from Gustavsson et al.,[57]

TABLE 5: Experimental[31] and Calculated (APM) Stokes Shifts and Widths Relative to 2-methylbutane (10^3 cm^{-1})

	experimental[31]			calculated					
solvent	$\Delta\bar{\nu}_{st}$[a]	σ_{abs}[b]	σ_{em}[c]	$\Delta\bar{\nu}_{st}$[a]	σ_{abs}[b]	σ_{em}[c]	$\Delta\bar{\nu}_{st}$[d]	σ_{abs}[d]	σ_{em}[d]
toluene	0.26	0.06	−0.17	0.41	0.58	0.43	0.45	0.61	0.51
benzene	0.41	−0.06	−0.41	0.49	0.58	0.43	0.56	0.73	0.67
p-xylene	0.44	0.06	0.59	0.28	0.41	0.31	0.30	0.43	0.31
chloroform	0.49	0.19	−1.02	0.48	0.67	0.43	0.53	0.73	0.67
dichlormethane	0.70	0.13	−1.02	0.79	0.93	0.55	0.94	1.09	0.98
tetrahydrofuran	0.98	0.84	−0.12	1.00	1.10	0.45	1.23	1.34	1.19
methyl acetate	1.19	1.37	−0.06	1.01	1.19	0.49	1.23	1.34	1.19
acetone	1.36	1.10	−0.46	1.29	1.46	0.17	1.68	1.77	1.36
nitromethane	1.37	1.50	−1.14	1.40	1.64	−0.38	1.91	2.08	1.36
dimethyl sulfoxide	1.35	1.64	−0.35	1.38	1.73	−0.56	1.91	2.14	1.30
acetonitrile	1.67	1.50	−0.63	1.39	1.64	−0.21	1.86	2.02	1.41

[a] Relative to the Stokes shift in 2-methylbutane. [b] Calculated as $[\beta(\Gamma_{abs}^2 - \Gamma_{ref}^2)]/[8 \ln 2]$, where Γ_{ref} is the spectral width in 2-methylbutane. [c] Calculated as $[\beta(\Gamma_{em}^2 - \Gamma_{ref}^2)]/[8 \ln 2]$. [d] Calculated neglecting the solvent−vibrational coupling, as in eq 54.

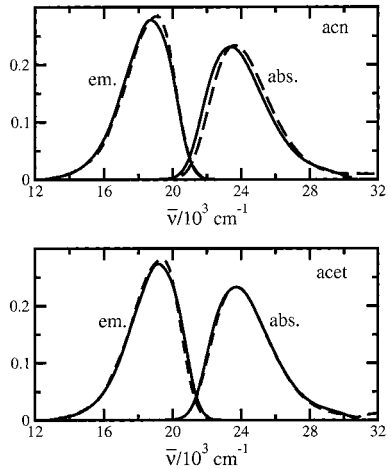

Figure 8. Normalized experimental[31] (dashed lines) and calculated (solid lines) spectra for absorption (abs.) and emission (em.) in acetonitrile (acn) and acetone (acet).

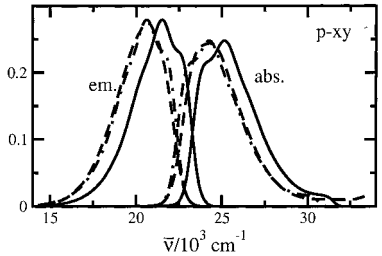

Figure 9. Same as in Figure 8, but with *p*-xylene (*p*-xy) as the solvent. The dot−dashed spectra are obtained by a uniform shift of the calculated spectra by −900 cm^{-1}.

and from Rechthaler and Köhler,[52] suggests that the emission width is essentially constant or decreases slightly with increasing solvent polarity and the absorption width increases with increasing solvent polarity.

To within experimental uncertainties, our present calculations are in accord with the data given by Reynolds et al.[31] (Figures 8−10, Table 5). Both emission and absorption experimental spectra are excellently reproduced for polar acetonitrile and acetone (Figure 8), but there is an insufficient red shift in the calculations for *p*-xylene (Figure 9). We should remind at this point that the dispersion spectral shift (E_i^{disp} in eq 12), which does not affect the Stokes shift,[41] is not included in the present calculations. This shift component is proportional to the solvent Lennard−Jones (LJ) energy, ϵ_{LJ}, and is small for acetone and acetonitrile ($\epsilon_{LJ}/k_B = 296$ K for acetone[58]). For *p*-xylene with $\epsilon_{LJ}/k_B = 725$ K[58] (the highest LJ energy among the solvents in

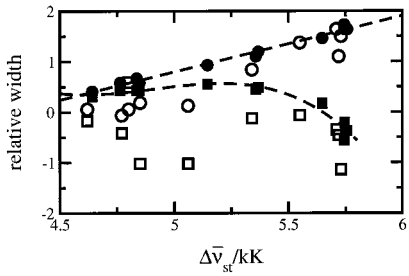

Figure 10. Experimental (open points) and calculated (APM, closed points) width for absorption (circles) and emission (squares) relative to the absorption and emission width in 2-methylbutane (see Table 5) vs the total Stokes shift. Dashed lines are regressions drawn through the filled points as a guide for the eye.

Table 1), the dispersion spectral shift may be more significant, which is reflected by an insufficient red shift of calculated spectral lines. This viewpoint is supported by the fact that a good agreement between the calculated and experimental spectra is achieved by a uniform shift of both calculated spectra by −900 cm^{-1} (dot−dashed lines in Figure 9). A part of the red-shift mismatch may arise from the solute quadrupole not taken into account in the present calculations. However, an absence of a considerable discrepancy between the calculated and experimental Stokes shift suggests that, even if important in each of the chromophore's states, the quadrupole moment does not change significantly with excitation. Furthermore, a good agreement between the calculated and experimental spectra in polar solvents points to a more probable effect of dispersion forces responsible for the red shift. Note also that, by adopting the experimental energy $\bar{\nu}_m^{ref}$ in eq 29, the dispersion stabilization in 2-methylbutane is included in our calculations. Only substantial deviations from that value should generate a noticeable uniform shift of the calculated spectra.

The solvent dependence of the overall Stokes shift is reproduced for a broad range of solvent polarities, from nondipolar to strongly polar solvents. The absorption width agrees well with the experiment, and the change of the emission width relative to 2-methylbutane is negative in strongly polar solvents, a feature seen in experiment (Figure 10). The present calculations, however, do not yield a negative shift of the emission width relative to 2-methylbutane in nondipolar and weakly polar solvents: the overall emission width shows a maximum similar to but less pronounced than that seen for the band shape due only to solvent (Figure 6). The last three columns in Table 5 list the Stokes shifts and widths calculated by neglecting the solvent−vibration coupling induced by electron delocalization ($\Delta\tau^{\pm} = 1$ in eq 45). They are therefore

obtained through the convolution of the reference spectral band in 2-methylbutane with the solvent-induced band (eq 54), both considered as independent of each other. The difference of about 40% between the Stokes shifts calculated with account for the coupling between the vibrational and solvent modes and without this coupling in highly polar solvents accounts for the delocalization-induced decrease in the vibrational Stokes shift (see Discussion below). Also, no negative shift of the emission width with respect to 2-methylbutane can be obtained unless the solvent−vibrational coupling is turned on.

4. Discussion

4.1. Model. The classical models of radiative and radiationless transitions in condensed phases usually operate in the framework of one basic scheme that separates the transition probability into two factors: coupling between the electronic states and a FC factor (FCWD) defining the statistical probability of bringing the two electronic states in resonance or to generate an energy gap equal to the photon energy.[1,4,9−12] When dipolar optical transitions are considered, the transition dipole is responsible for the electronic coupling effects. The transition dipole interacts with the external electric field of the radiation, $\mathbf{E}_0(t)$, leading to dipolar optical transitions caused by the interaction perturbation

$$-\mathbf{m}_{0,12}\cdot\mathbf{E}_0(t) \tag{58}$$

A perturbation treatment to the first order in this interaction then leads to the following general form for the absorption and emission intensities:[59]

$$I_{\mathrm{abs/em}} \propto |m_{0,12}|^2 \mathrm{FCWD}_{\mathrm{abs/em}} \tag{59}$$

Here, the FCWD depends solely on diagonal matrix elements of the Hamiltonian and is independent of any off-diagonal matrix elements.

When a chromophore is placed into a solvent, the interaction with the solvent reaction fields adds to the interaction with the external field

$$-\mathbf{m}_{0,12}\cdot\mathbf{R} \tag{60}$$

Since the local molecular field **R** can be very strong, much exceeding the external radiation field $\mathbf{E}_0(t)$, we cannot generally use a perturbation expansion in the interaction in eq 60. This term is therefore retained in the FCWD.[60] As a result, the FCWD of an intense optical transition in polar liquids includes a dependence on the transition dipole and the general form of transition intensity should be changed to

$$I_{\mathrm{abs/em}} \propto |m_{0,12}|^2 \mathrm{FCWD}_{\mathrm{abs/em}}(|m_{0,12}|) \tag{61}$$

The interaction term in eq 60 is responsible for mixing of the orthogonal gas-phase adiabatic states changing the electronic occupation numbers ($n^{\pm}$) of the ground and excited states. These occupation changes are damped by virtual transitions to other excited states when $\Delta\alpha_0 > 0$. An opposite effect of enhancement of delocalization by polarizability change occurs when $\Delta\alpha_0 < 0$ (this may be achieved in photoexcited CT). Since the coupling of electronic states to intramolecular vibrations is proportional to the electronic occupation number ($n^{\pm}$),[6] electronic delocalization distorts the vibronic envelope, squeezing and shifting the absorption and emission lines closer to each other. All three of these effects combine to produce the optical bands calculated here for 11 solvents ranging in polarity from nondipolar to strongly polar.

The present model leads to a breakdown of the linear relation between the spectral width and the Stokes shift (eq 3). The origin of this effect is the intrinsic nonlinearity (generated by chromophore's polarizability and electronic delocalization) of the coupling of the electronic subsystem to the nuclear modes. Noteworthy is that this effect arises despite the fact that the neat solvent is characterized by Gaussian fluctuations of its electric field. The energy gap fluctuations are non-Gaussian, in contrast to systems with fixed molecular charges.[21c] The change in statistics is caused by a nonlinear dependence of the instantaneous solute energy on the solvent field. It is reflected in the transformation from a parabolic to a linear free energy gap law for activated processes,[29] in a nonlinear squeezing of optical bands for charge delocalized systems,[60] and in transient bandwidths in time-resolved optical experiments.[61] The solvent progression of the inhomogeneous bandwidth obtained here (Figure 6) is a manifestation of these nonlinear effects. It is instructive to look deeper in the origins of this phenomenon.

4.2. Spectral Width. The prediction of a nonmonotonic (passing through a maximum) polarity dependence of the emission width is one of the central outcomes of the present model. The standard interpretation of the spectral width is based on the widely used picture of two displaced parabolic free energy surfaces between which optical transitions occur. In this picture, the width of the spectral distribution is directly related to the parabolas' curvatures: the more shallow the free energy surface (smaller the curvature) is, the larger the width produced by thermal fluctuations of the solvent will be. For a dipolar solute, fluctuations of its electronic energy levels occur due to thermal fluctuations of the reaction field and the relation between the spectral width and the curvature of the free energy surface in the parabolic approximation is given by the following mathematical relation:[20c,21b,62b]

$$\beta\sigma_{\pm}{}^2 = \Delta\tilde{m}_0{}^2[\partial^2 E^{\pm}/\partial R_{\|}{}^2]^{-1}|_{R_{\|}=R_{\|}^{\mathrm{eq}},R_{\perp}=0} \tag{62}$$

The second derivative of the free energy $E^{\pm}(R_{\|},R_{\perp})$ is taken at the point of equilibrium $\{R_{\|}^{\mathrm{eq}},0\}$, where $\partial E^{\pm}(R_{\|},0)/R_{\|} = 0$. If this definition of the spectral width is used for the data shown in Figure 6, the second derivative of the excited free energy surface should pass through a minimum as a function of solvent polarity. This actually does not happen.

The diabatic, two-parabolas approximation for the CT free energy surfaces is not applicable to spectral modeling in electronically delocalized systems, and a nonmonotonic solvent dependence of the emission width is an excellent demonstration of this fact. The adiabatic splitting between the free energy surfaces results in the major difference with the diabatic case that there is a minimum energy gap between the free energy surfaces. This fact, not very important for small electronic overlap, becomes a crucial factor affecting spectral widths in systems with strong electronic overlap. Light with energy less than that of the minimum splitting ($\bar{\nu}_{\min}$ in Figure 11) cannot be absorbed. Therefore, spectral intensity is zero at $\bar{\nu} < \bar{\nu}_{\min}$. Accordingly, when an optical band shifts closer to the boundary $\bar{\nu}_{\min}$ ($\bar{\nu}_{\mathrm{abs/em}} \simeq \bar{\nu}_{\min}$), its red wing narrows because of the proximity of the limiting frequency (Figure 11, lower panel). Since emission lines are more red-shifted than the absorption lines, they are closer to the limiting frequency (Figures 11 and 12, lower panels) and are more strongly affected by the existence of the limiting frequency. As a result, a nonlinear line squeezing builds up for emission lines, compensating for broadening

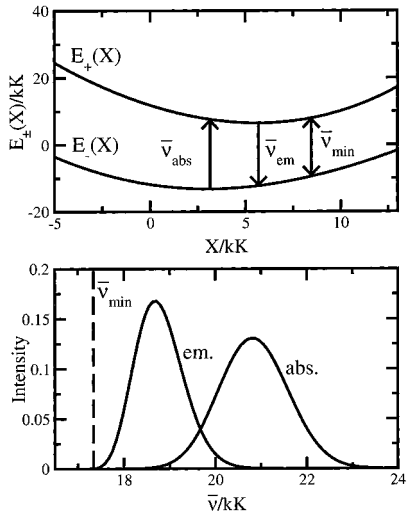

Figure 11. Upper panel: upper ($E^+(X)$) and lower ($E^-(X)$) free energy surfaces as functions of the reaction coordinate $X = \Delta\tilde{m}_0 R_{||}$. The absorption, emission, and minimal energy gaps are indicated. Lower panel: absorption and emission solvent-induced spectral line-shapes corresponding to the transitions shown in the upper panel. The dashed line indicates the position of the minimal transition frequency. Calculations are for C153 in acetonitrile.

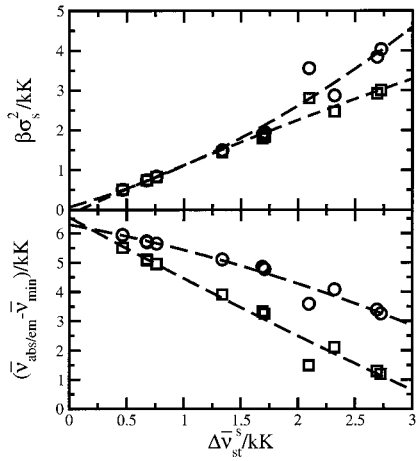

Figure 12. Upper panel: spectral width for absorption (circles) and emission (squares) according to eq 62 vs the solvent-induced Stokes shift. Lower panel: absorption (circles) and emission (squares) first moments minus the minimum transition energy (see Figure 11). Points indicate the solvents listed in Table 1 (excluding 2-methylbutane). The dashed lines are regressions drawn as a guide for the eye.

caused by increasing solvation power at higher polarities. Analogous effects are responsible for asymmetry of optical absorption bands in mixed-valence CT complexes.[60,63,64]

This is the reason the definition of the width through the free energy curvature at the coordinate of its minimum does not have any bearing on the observed width. Figure 12 (upper panel) shows the dependence of the width $\beta\sigma_\pm^2$, defined in termed of free energy curvature (eq 62), on the solvent-induced Stokes shift for 11 solvents listed in Table 1. [The free energy surfaces are given by eqs 16 and 17; we neglect here the solvent−vibrational coupling ($\Delta\tau^\pm = 1$) in order to emphasize the solvent width component.] As is seen, the widths generated for absorption and emission are very close to each other on one hand, and their polarity dependence is monotonic on the other. This indicates that the passing of the emission width through a maximum is not caused by a change in the curvature of the free energy surface at its minimum. The free energy surface is essentially nonparabolic, and the maximum is a result of

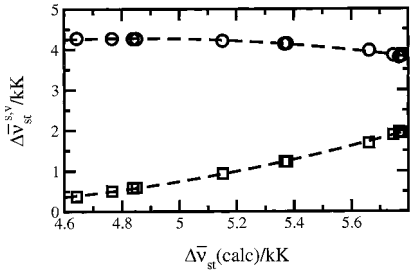

Figure 13. Solvent Stokes shift (squares, $\Delta\bar{\nu}_{st}^s$, Table 1) and the vibrational Stokes shift ($\Delta\bar{\nu}_{st}^v$, circles) vs the total APM Stokes shift. The vibrational Stokes shift is obtained by subtracting the calculated solvent component from the total calculated Stokes shift. Lines are regressions through the points.

nonlinear squeezing of the red wing of the band, with a resulting narrowing of the overall bandwidth of the intensity at half-height. The lower panel in Figure 12 shows that the emission line gets very close to the limiting frequency $\bar{\nu}_{min}$ in polar solvents, and this fact explains the appearance of the maximum in the solvent dependence of the emission width.

4.3. Polarizability versus Delocalization. Optical transitions in polarizable chromophores are affected by two physically important factors: mixing of the adiabatic states involved in the transition (through the transition dipole) and overall polarizability of the chromophore. These two effects are actually a reflection of the same physical picture: coupling of the electronic states results in redistribution of electronic density between them. If the extent of density redistribution is coupled to the solvent, the system gains intrinsic nonlinearity, as reflected by the spectral features considered here. Both the Stokes shift and the spectral width are sensitive to the details of coupling between the electronic states. A positive polarizability shift ($\Delta\alpha_0 > 0$) gives rise to a wider emission line. On the other hand, a nonzero transition dipole generates narrowing of the emission line. The overall solvent-induced spectral width is the result of compensation between these two effects. The narrowing due to electron delocalization is stronger than the broadening due to polarizability for emission, leading to narrower emission lines relative to absorption lines (Figure 4).

4.4. Solvent−Vibrational Coupling. We achieved a quantitative account of the solvent dependence of both the Stokes shift and the spectral width observed for C153. The calculations reproduce a negative change of the total (solvent and vibrational) emission width with increasing solvent polarity. This result comes about from the explicit inclusion of the coupling of solvent nuclear reaction field and vibrational modes of the chromophore generated by electronic delocalization. The qualitative outcome of this analysis is that the vibrational reorganization energy, when calculated according to eq 1, is solvent-dependent (Figure 13). This effect was anticipated in some previous publications.[3b,65,66] As is seen in Table 5, the omission of the solvent dependence of the vibrational reorganization energy leads to much higher values for absorption and emission bandwidths.

Not only the width, but also the overall Stokes shift is affected by the solvent−vibrational coupling. It amounts to up to 40% overestimate of the Stokes shift in strongly polar solvents (Table 5). This result has an important bearing on the problem of the relative contribution of quadrupolar solvation to nuclear reorganization recently raised in the literature.[31,34] As is seen from Table 5, the experimental Stokes shift (relative to 2-methylbutane) changes by a factor of 3 when passing from benzene to dmso. This change is much more moderate than could be

expected from dielectric cavity models, and it has been ascribed to quadrupolar solvation in nondipolar solvents neglected by dielectric models.[31,34] However, such a moderate variation of the Stokes shift with solvent polarity is also hard to explain within the molecular model employed here, which explicitly incorporates solvent quadrupoles.[35] As is seen from Table 1, the solvent component of the Stokes shift changes more strongly with increasing solvent polarity than is seen for the overall Stokes shift (open points in Figure 2). The puzzle is resolved by the present model, which shows that the increase in the solvent Stokes shift is partially compensated by a decrease of the vibrational Stokes shift due to electronic delocalization effects (Figure 13). Note that similar effects may be important in treating the dynamic solvent response that should include the solvent-driven decay of the vibrational Stokes shift along with the traditionally considered time-dependent solvent Stokes shift.

4.5. Spectral Modeling. The present model is designed to generate spectra in polar solvents from solute charge distribution, polarizability, and experimental spectra measured in a reference, nonpolar solvent. The latter feature is incorporated to avoid the necessity to calculate often complex vibrational envelopes of large optical dyes. Several novel effects turned out to be important for an accurate description of the solvent dependence of the first two spectral moments of C153. Not all of them should necessarily be included in the spectral analysis of other chromophores. Here we estimate relative importance of various contributions.

The solvent−vibrational coupling presents the main complexity to the present analysis. Its importance can be estimated from the change in the Stokes shift due to the vibrational−solvent coupling $\delta\bar{\nu}_i = \lambda_v|\Delta\tau^+ + \Delta\tau^- - 2|$. In many practical cases, the off-diagonal contribution $V_{12}[\mathbf{R}_p]$ to the instantaneous adiabatic energy gap $\Delta E[\mathbf{R}_p,\mathbf{q}]$ is small compared to $\Delta E_{0s}[\mathbf{R}_p,\mathbf{q}]$ (eq 17). Expansion of $\Delta\tau^{\pm}$ in $V_{12}[\mathbf{R}_p]/\Delta E_{0s}[\mathbf{R}_p,\mathbf{q}]$ yields for the Stokes shift components due to the vibrational−solvent coupling

$$\delta\nu_i \simeq 8(a_p m_{0,12} m_{0i})^2 \frac{\Delta\bar{\nu}_{st}^{ref}}{\bar{\nu}_{abs/em}^2} \tag{63}$$

For C153 in acetonitrile, the above equation gives 300 cm^{-1}, on the same order as the difference of 460 cm^{-1} between columns 7 and 8 in Table 5. Because of a large vibrational Stokes shift and a large transition dipole, the vibrational−solvent coupling becomes important for modeling the solvent dependence of the overall Stokes shift of C153. This component will be less important for chromophores with smaller vibrational reorganization energy and/or smaller transition dipoles. The effect of vibrational−solvent coupling is scaled with the energy gap $\bar{\nu}_{abs/em}^2$ in eq 63. The energy gap, large for UV transitions in C153, is usually much smaller when the electronic density is delocalized between a CT state and a locally excited state of the donor−acceptor complex. The solvent−vibrational coupling should be more important in such systems.[66]

Effects of polarizability variation and electronic delocalization are expected to be more abundant than solvent−vibrational coupling in optical spectroscopy. Figure 4 shows that correct modeling of the solvent-induced shift and width on emission lines demands inclusion of both effects. On the other hand, the absorption line shape is well modeled within the DPM. This simplified, analytical version of the model can be used for absorption lines. Note also that emission lines are not dramatically different from the prediction of the DPM as well. They can be modeled by adopting an effective polarizability of the excited state. To summarize, the present model provides a convenient theoretical framework for spectral modeling that goes beyond the Marcus−Hush picture. The present analysis includes two independent components: equilibrium solvation and spectral band shapes. The model is formulated in terms of linear solvation response coefficients which can be calculated in any appropriate solvation model. Depending on the chromophore and transitions considered, the spectral analysis may be based on a hierarchy of approximations: DPM, APM, or APM combined with the vibrational−solvent coupling.

5. Conclusions

This study is a step toward deeper understanding of the optical band shape in condensed phases, yielding a self-consistent account of the solvent variation of both the position and the width of a spectral line. We have developed a band-shape analysis of optical lines of polarizable chromophores, which accommodates transitions involving a variable degree of electronic delocalization. The theory is used to reproduce experimental band shapes of the coumarin-153 dye in a broad range of solvents from nondipolar to strongly polar. The major result of the analysis is a qualitative difference in solvent progressions of optical widths for absorption and emission. The solvent-induced absorption width increases with the Stokes shift and the solvent-induced emission width goes through a maximum with increasing Stokes shift. The total spectral width of emission transitions essentially reproduces this trend. The present model demonstrates that inclusion of the transition dipole in the FC factor of an optical or radiationless transition is a necessary component of a correct description of optical band shapes and radiationless rates between strongly coupled electronic states.

Acknowledgment. We are grateful to Prof. N. P. Ernsting and Prof. M. Maroncelli for sending us experimental spectra of C153 and useful comments and suggestions on the manuscript. The authors acknowledge support through the startup fund by the Department of Chemistry and Biochemistry at ASU and the donors of the Petroleum Research Fund, administered by the American Chemical Society (36404-G6) (D.V.M.) and DE-AC02-98CH10886 at Brookhaven National Laboratory (M.D.N.).

Appendix A: Solvent Response Coefficients

The Padé approximation represents the solvent response function as a ratio of polynomials of two polarity densities, y_d and y_q.[35,49] The density of polarizable dipoles of the solvent

$$y_d = (4\pi/9)\beta\rho(m')^2 + (4\pi/3)\alpha\rho \tag{A1}$$

depends on the effective dipole moment of the solvent molecules in the liquid (m'), and the solvent polarizability (α); m' is calculated from the corresponding gas-phase values (Table 1) using the Wertheim self-consistent approach.[67] Similarly, the density of solvent quadrupoles is defined by the relation[35]

$$y_q = (2\pi/5)\beta\rho Q^2/\sigma^2 \tag{A2}$$

where we neglect the quadrupolar polarizability of the solvent molecules.

With liquid-state dipolar and quadrupolar densities defined in this manner, the Padé approximant for the total response function in eq 52 is given by the following expression

$$P(m,q,\alpha) = \frac{y_d + (I_6^{(2)}/I_4^{(2)})y_q}{1 + f^{(3)}/f^{(2)}} \quad \text{(A3)}$$

with

$$f^{(2)} = y_d I_4^{(2)} + y_q I_6^{(2)} \quad \text{(A4)}$$

$$f^{(3)} = y_d{}^2 \kappa_d I_{DDD}^{(3)} + y_d y_q \kappa_{dq} I_{DDQ}^{(3)} + y_q{}^2 \kappa_q I_{DQQ}^{(3)} \quad \text{(A5)}$$

In the above equations, $I_4^{(2)}$ and $I_6^{(2)}$, depending only on the reduced solvent density $\rho^* = \rho\sigma^3$ and the solute−solvent size ratio R_0/σ, are two-particle perturbation integrals obtained by direct perturbation expansion of the chemical potential in the solute−solvent interaction potential ($R_{\text{eff}}{}^3 = \sigma^3/I_4^{(2)}$). The three-particle perturbation integrals $I^{(3)}$ also depend on the reduced solvent density ρ^* and R_0/σ; the correction factors $\kappa_{d,q,dq}$ are introduced to bring the results of the analytical theory in agreement with computer simulations. They depend on R_0/σ only. All the parameters used in eqs A3−A5 are tabulated in refs 28 and 33a.

Separation of the total solvent response

$$P(m,q,\alpha) = P_d(m,q,\alpha) + P_q(m,q,\alpha) \quad \text{(A6)}$$

into the components arising from dipolar, $P_d(m,q,\alpha)$, and quadrupolar, $P_q(m,q,\alpha)$, solvation mechanisms is achieved by noting that, in linear response, the solvation chemical potential is one-half of the average solute−solvent interaction energy.[49c] One can then use the equations for average dipolar and quadrupolar solute−solvent interaction energies given in ref 35. This procedure yields

$$P_d(m,q,\alpha) = \frac{2y_d + 2y_d{}^2 \kappa_d I_{DDD}^{(3)}/I_4^{(2)} + y_d y_q \kappa_{dq} I_{DDQ}^{(3)}/I_4^{(2)}}{2(1 + f^{(3)}/f^{(2)})^2} \quad \text{(A7)}$$

and

$$P_q(m,q,\alpha) = \frac{2y_q I_6^{(2)} + 2y_q{}^2 \kappa_q I_{DQQ}^{(3)} + y_d y_q \kappa_{dq} I_{DDQ}^{(3)}}{2I_4^{(2)}(1 + f^{(3)}/f^{(2)})^2} \quad \text{(A8)}$$

Note that one cannot obtain, e.g., the dipolar solvation component by assuming $y_q = 0$ in eq A3. This happens because the dipolar and quadrupolar components of the solvent response are highly intermingled due to dipole−quadrupole correlations between the solvent molecules.

Appendix B: Diabatic and Two-State Approximations

The integral over the transverse reaction field $R_\perp$ in eq 45 leads to analytical expressions for the solvent-induced line-shape in two limiting cases of the DPM and TSM. In the former case, the solvent-induced inhomogeneous broadening results in the band-shape function[29]

$$\text{FCWD}_{\text{abs/em}}^{\text{s}}(\bar{\nu}) = A_i \sqrt{\frac{\lambda_i |\alpha_i|^3}{|\bar{\nu} - X_0|}} e^{-\beta(|\alpha_i||\bar{\nu} - X_0| + \lambda_i \alpha_i{}^2)} I_1(2\beta\sqrt{|\alpha_i|^3 \lambda_i |\bar{\nu} - X_0|}) \quad \text{(B1)}$$

where $I_1(x)$ is the first-order modified Bessel function and A_i is the normalization factor

$$A_i = (1 - e^{-\beta\lambda_i\alpha_i{}^2})^{-1} \quad \text{(B2)}$$

Equation 1 sets up two band shapes ($i = 1$ for absorption and $i = 2$ for emission), each characterized by three parameters: α_i, λ_i, and X_0. The parameters λ_i are solvent reorganization energies for absorption and emission of a chromophore with different polarizabilities in the ground and excited states. They are not equal because of a quadratic solute−solvent coupling in the instantaneous energy gap caused by a nonzero polarizability shift of the chromophore.[29] The parameters $\alpha_i(\alpha_2 = 1 + \alpha_1)$ determine the extent of deviation of the inhomogeneous band from a Gaussian band; a Gaussian band shape is recovered in the limit $\alpha_1 \to \infty$.

The reorganization energies λ_i are related to each other through the non-Gaussian parameter α_1 as follows:[68]

$$\alpha_1{}^3 \lambda_1 = (1 + \alpha_1)^3 \lambda_2 \quad \text{(B3)}$$

The parameter X_0 defines the boundary of the band of optical excitations for which nonzero spectral intensities exist (analogously to $\bar{\nu}_{\min}$ in Figure 11). It is related to the gas-phase energy gap between initial and final states, the dispersive and induction stabilization free energies, and the differences in the dipole moment and polarizability through the equation

$$X_0 = \Delta E + \Delta E^{\text{disp}} + \Delta F^{\text{ind}} + \frac{\Delta \tilde{m}_0{}^2}{2\Delta\tilde{\alpha}_0} \quad \text{(B4)}$$

In the TSM, there is no dependence of the instantaneous energy surfaces on the transverse field component and the integral in eq 45 becomes[60]

$$\text{FCWD}_{\text{abs/em}}^{\text{s}}(\bar{\nu}) = \sum_k \frac{4\pi a_{\text{p}}}{\beta Q^{\mp} \Delta E'[R_{||}^{(k)}]} \text{ or } \beta(4a_{\text{p}})^{-1}(R_{||}^{(k)})^2 \times \exp(-\beta(R_{||}^{(k)})^2/4a_{\text{p}} - \beta E^{\mp}[R_{||}^{(k)}]) \quad \text{(B5)}$$

where the sum now runs over the two roots of the second-order polynomial equation $\Delta E[R_{||}^{(k)}] = \bar{\nu}$.

References and Notes

(1) (a) Mataga, N.; Kubota, T. *Molecular Interactions and Electronic Spectra*: Marcel Dekker: New York, 1970. (b) Lax, M. *J. Chem. Phys.* **1952**, *20*, 1752. (c) Kubo, R.; Toyozawa, Y. *Prog. Theor. Phys.* **1955**, *13*, 160. (d) Englman, R.; Jortner, J. *Mol. Phys.* **1970**, *18*, 145.

(2) (a) Pekar, S. I. *Research in Electron Theory of Crystals*; USAEC: Washington, DC, 1963. (b) Gehlen, J. N.; Chandler, D. Kim, H. J.; Hynes, J. T. *J. Phys. Chem.* **1992**, *96*, 1748. (c) Kim, H. J.; Hynes, J. T. *J. Chem. Phys.* **1992**, *96*, 5088. (d) Matyushov, D. V.; Ladanyi, B. M. *J. Chem. Phys.* **1998**, *108*, 6362. (e) Matyushov, D. V.; Ladanyi, B. M. *J. Phys. Chem. A* **1998**, *102*, 5027.

(3) (a) Tomasi, J.; Cammi, R.; Mennucci, B. *Int. J. Quantum Chem.* **1999**, *75*, 783. (b) Matyushov, D. V.; Schmid, R.; Ladanyi, B. M. *J. Phys. Chem. B* **1997**, *101*, 1035. (c) Grozema, F. C.; van Duijnen, P. Th. *J. Phys. Chem. A* **1998**, *102*, 7984.

(4) (a) Barbara, P. F.; Jarzeba, W. *Adv. Photochem.* **1990**, *15*, 1. (b) Barbara, P.; Meyer, T. J.; Ratner, M. A. *J. Phys. Chem.* **1996**, *100*, 13148. (c) Myers, A. B. *Annu. Rev. Phys. Chem.* **1998**, *49*, 267.

(5) Matyushov, D. V.; Voth, G. A. *J. Phys. Chem. A* **2000**, *104*, 6470.

(6) For a given normalized state, the occupation numbers (populations) of the two vacuum adiabatic basis states, ψ_1 (ground) and ψ_2 (excited), are denoted n_1 and n_2, where $n_1 + n_2 = 1$. The two states mix in solution due to the interaction of the transition dipole with the solvent reaction field. The new state diagonalizing the Hamiltonian matrix then refer to the lower ("−") and upper ("+") CT surfaces. The change in occupations in the transition from the lower to the upper state is then defined as $\Delta n = n_1(\text{lower}) - n_2(\text{upper})$.[5] Hence, for the vacuum adiabatic states, $\Delta n = +1$. In the present case of C153, the adiabatic vacuum states are reasonably well localized (i.e., they do not differ strongly from the diabatic charge-localized states one might define, for example, on the basis of Mulliken−Hush theory[26]), and their mixing due to interaction of the vacuum transition dipole moment and the solvent reaction field in solution will tend to delocalize the charge distribution.

(7) (a) Marcus, R. A. *J. Chem. Phys.* **1965**, *43*, 1261. (b) Marcus, R. A. *Annu. Rev. Phys. Chem.* **1964**, *15*, 155.

(8) We consider here line broadening only due to a statistical distribution of solvent configurations around the solute (inhomogeneous broadening). The broadening due to finite lifetime of electronic excited states (homogeneous broadening) is neglected on the assumption that the solute−solvent interaction is so strong that $c\sigma_{abs/em}\tau_s \gg 1$, where c is the speed of light and τ_s is a characteristic solvent relaxation time [see, e.g.: Stephens, M. D.; Saven, J. G.; Skinner, J. L. *J. Chem. Phys.* **1997**, *106*, 2129]. On the other hand, we assume homogeneous solvent dynamics, i.e., $\tau_s \ll \tau_{exp}$, where τ_{exp} is the experimental time scale, e.g., the lifetime of the excited state. Solvent dynamic heterogeneity gains importance in supercooled liquids.[22c]

(9) (a) Hush, N. *Progr. Inorg. Chem.* **1967**, *8*, 391. (b) Marcus, R. A. *J. Phys. Chem.* **1989**, *93*, 3078.

(10) Bixon, M.; Jortner, J. *Adv. Chem. Phys.* **1999**, *106*, 35.

(11) (a) Kjaer, A. M.; Ulstrup, J. *J. Am. Chem. Soc.* **1987**, *109*, 1934. (b) Walker, G. C.; Åkesson, E.; Johnson, A. E.; Levinger, N. E.; Barbara, P. F. *J. Phys. Chem.* **1992**, *96*, 3728. (c) Gould, I. R.; Noukakis, D.; Gomez-Jahn, L.; Goodman, J. L.; Farid, S. *J. Am. Chem. Soc.* **1993**, *115*, 4405. (d) Cortés, J.; Heitele, H.; Jortner, J. *J. Phys. Chem.* **1994**, *98*, 2527. (e) Morais, J.; Zimmt, M. B. *J. Phys. Chem.* **1995**, *99*, 8863.

(12) Chan, P.; Meyer, T. J. *Chem. Rev.* **1998**, *98*, 1439.

(13) $\langle(\delta\bar{\nu})^2\rangle$ are, strictly speaking, spectral cumulants. We use the term spectral moment to comply with traditional spectroscopic terminology.

(14) In the present paper, we confine the consideration by the case when the normal coordinates are invariant with the transition. Duschinskii rotation[36a] of normal modes breaks down the equality of absorption and emission widths for vibrational modes.

(15) (a) Newton, M. D. *Chem. Rev.* **1991**, *91*, 767. (b) Newton, M. D. *Adv. Chem. Phys.* **1999**, *106*, 303.

(16) (a) Gustavsson, T.; Baldacchino, G.; Mialocq, J.-C.; Pommeret, S. *Chem. Phys. Lett.* **1995**, *236*, 587. (b) van der Meulen, P.; Jonkman, A. M.; Glasbeek, M. *J. Phys. Chem. A* **1998**, *102*, 1906. (c) Nagarajan, V. *Chem. Phys. Lett.* **2000**, *317*, 203.

(17) (a) Painelli, A.; Terenziani, F. *Chem. Phys. Lett.* **1999**, *312*, 211. (b) Painelli, A.; Terenziani, F. *J. Phys. Chem. A* **2000**, *104*, 11041. (c) Terenziani, F.; Painelli, A.; Comoretto, D. *J. Phys. Chem. A* **2000**, *104*, 11049.

(18) Horng, M. L.; Gardecki, J. A.; Papazyan, A.; Maroncelli, M. *J. Phys. Chem.* **1995**, *99*, 17311.

(19) Köhler, G.; Rechthaler, K.; Grabner, G.; Luboradzki, R.; Suwińska, K.; Rotkiewicz, K. *J. Phys. Chem. A* **1997**, *101*, 8518.

(20) (a) Kuharski, R. A.; Bader, J. S.; Chandler, D.; Sprik, M.; Klein, M. L.; Impey, R. W. *J. Chem. Phys.* **1988**, *89*, 3248. (b) King, G.; Warshel, A. *J. Chem. Phys.* **1990**, *93*, 8682. (c) Yelle, R. B.; Ichiye, T. *J. Phys. Chem. B* **1997**, *101*, 4127.

(21) (a) Maroncelli, M. *J. Chem. Phys.* **1991**, *94*, 2084. (b) Carter, E. A.; Hynes, J. T. *J. Chem. Phys.* **1991**, *94*, 5961. (c) Geissler, P. L.; Chandler, D. *J. Chem. Phys.* **2000**, *113*, 9759.

(22) (a) Shemetulskis, N. E.; Loring, R. F. *J. Chem. Phys.* **1991**, *95*, 4756. (b) Matyushov, D. V.; Ladanyi, B. M. *J. Chem. Phys.* **1997**, *107*, 1375. (c) Richert, R. *J. Chem. Phys.* **2000**, *113*, 8404.

(23) Zhou, H.-X.; Szabo, A. *J. Chem. Phys.* **1995**, *103*, 3481.

(24) Fonseca, T.; Ladanyi, B. M. *J. Mol. Phys.* **1994**, *60*, 1.

(25) (a) Re, M.; Laria, D. *J. Phys. Chem. B* **1997**, *101*, 10494. (b) Graf, P.; Nitzan, A. *Chem. Phys.* **1998**, *235*, 297. (c) Yamaguchi, T.; Kimura, Y.; Hirota, N. *J. Chem. Phys.* **1999**, *111*, 4169.

(26) Cave, R.; Newton, M. D. *Chem. Phys. Lett.* **1996**, *249*, 15.

(27) The delocalization parameter[5] $\Delta e = (1 + 4m_{0,12}^2/\Delta m_0^2)^{-1/2}$ is often used to quantify the extent of electronic density delocalization, where $m_{0,12}$ and Δm_0 are the adiabatic transition and difference dipole moments. This parameter is indeed very close to the difference in electronic occupation numbers for self-exchange reactions but increasingly deviates from the occupation difference with increasing equilibrium energy gap.[5] The parameter Δe thus cannot be used to characterize delocalization in the inverted region characteristic of CT transitions in C153 (Figure 3 in ref 5).

(28) Chowdhury, A.; Locknar, D. A.; Premvardhan, L. L.; Peteanu, L. A. *J. Phys. Chem. A* **1999**, *103*, 9614.

(29) Matyushov, D. V.; Voth, G. A. *J. Phys. Chem. A* **1999**, *103*, 10981.

(30) (a) Walker, G. C.; Barbara, P. F.; Doorn, S. K.; Dong, Y.; Hupp, J. P. *J. Phys. Chem.* **1991**, *95*, 5712. (b) Kulinowski, K.; Gould, I. R.; Myers, A. B. *J. Phys. Chem.* **1995**, *99*, 9017. (c) Britt, B. M.; McHale, J. L.; Friedrich, D. M. *J. Phys. Chem.* **1995**, *99*, 6347. (d) Zong, Y.; McHale, J. L. *J. Chem. Phys.* **1997**, *106*, 4963.

(31) Reynolds, L.; Gardecki, J. A.; Frankland, S. J. V.; Horng, M. L.; Maroncelli, M. *J. Phys. Chem.* **1996**, *100*, 10337.

(32) Read, I.; Napper, A.; Zimmt, M. B.; Waldeck, D. H. *J. Phys. Chem. A* **2000**, *104*, 9385.

(33) Perng, B. C.; Newton, M. D.; Raineri, F. O.; Friedman, H. L. *J. Chem. Phys.* **1996**, *104*, 7153, 7177.

(34) Raineri, F. O.; Friedman, H. L. *Adv. Chem. Phys.* **1999**, *107*, 81.

(35) Matyushov, D. V.; Voth, G. A. *J. Chem. Phys.* **1999**, *111*, 3630.

(36) (a) Fischer, G. *Vibronic Coupling*; Academic Press: London, 1984. (b) At this level, the **Q**-dependence of the dipole moment ($\hat{\mathbf{m}}_0$) matrix elements is suppressed. The actual quantum mechanical electronic structure calculations were carried out at the S_0 ground-state equilibrium geometry (determined using the MNDO model[31]), thus defining $\mathbf{Q}_0$.

(37) (a) Bursulaya, B. D.; Zichi, D. A.; Kim, H. J. *J. Phys. Chem.* **1995**, *99*, 10069. (b) Ando, K. *J. Chem. Phys.* **1997**, *107*, 4585.

(38) Kim, H. J.; Bursulaya, B. D. *J. Chem. Phys.* **1998**, *108*, 3277.

(39) (a) Høye, J. S.; Stell, G. *J. Chem. Phys.* **1980**, *73*, 461. (b) Schweizer, K. S.; Chandler, D. *J. Chem. Phys.* **1983**, *78*, 4118. (c) Patey, G. N.; Levesque, D.; Weis, J. J. *Mol. Phys.* **1986**, *57*, 337.

(40) Mühlpfordt, A.; Schaz, R.; Ernsting, N. P.; Farztdinov, V.; Grimme, S. *Phys. Chem. Chem. Phys.* **1999**, *1*, 3209.

(41) We neglect the dependence of the dispersion shift on the solvent, excluding it from the energy gap. The dispersion shift is commonly fairly constant with solvent polarity,[3b] and the second moment over the solute−solvent dispersion coupling has a negligible contribution to the Stokes shift and spectral widths, see: Matyushov, D. V.; Schmid, R. *J. Chem. Phys.* **1995**, *103*, 2034. Because of this property, E^{disp} is the same for absorption and emission and is merely responsible for a uniform shift of both lines. Since our focus here on the Stokes shift and the width, the dispersion shift can be left out in considering the solvent effect on spectral band shapes.

(42) Gould, I. R.; Noukakis, D.; Gomez-Jahn, L.; Young, R. H.; Goodman, J. L.; Farid, S. *Chem. Phys.* **1993**, *176*, 439.

(43) The parameter $\Delta\tau^{\pm}$ is defined as analogous to the occupation number difference Δz in ref 5. The latter refers to the occupation numbers of the lower and upper CT surfaces at the corresponding equilibrium nuclear configurations, whereas $\Delta\tau^{\pm}$ is the "vertical" occupation number difference.

(44) Anisotropic polarizabilities from ab initio calculations (see footnote g in Table 2) were used to test the dependence of the calculated parameters on the solute's polarizability anisotropy. Anisotropic polarizability leads to a higher magnitude of the fitted solute radius but generates almost equivalent band shapes when the fitted radius is used.

(45) Schmid, R.; Matyushov, D. V. *J. Phys. Chem.* **1995**, *99*, 2393.

(46) Vath, P.; Zimmt, M. B.; Matyushov, D. V.; Voth, G. A. *J. Phys. Chem. B* **1999**, *103*, 9130.

(47) (a) Kumar, K.; Kurnikov, I. V.; Beratan, D. N.; Waldeck, D. H.; Zimmt, M. B. *J. Phys. Chem. A* **1998**, *102*, 5529. (b) Vath, P.; Zimmt, M. B. *J. Phys. Chem. A* **2000**, *104*, 2626. (c) Read, I.; Napper, A.; Kaplan, R.; Zimmt, M. B.; Waldeck, D. H. *J. Am. Chem. Soc.* **1999**, *121*, 10976.

(48) (a) Khajehpour, M.; Kauffman, J. F. *J. Phys. Chem. A* **2000**, *104*, 9512. (b) Kauffman, J. F. *J. Phys. Chem. A* **2001**, *105*, 3433.

(49) (a) Matyushov, D. V.; Schmid, R. *J. Chem. Phys.* **1996**, *105*, 4729. (b) Matyushov, D. V. *Chem. Phys.* **1996**, *211*, 47. (c) Matyushov, D. V.; Ladanyi, B. M. *J. Chem. Phys.* **1999**, *110*, 994.

(50) (a) Moyland, C. R. *J. Phys. Chem.* **1994**, *98*, 13513. (b) Lewis, J. E.; Maroncelli, M. *Chem. Phys. Lett.* **1998**, *282*, 197. (c) Smirnov, S. N.; Braun, C. L. *Rev. Sci. Instrum.* **1998**, *69*, 2875. (d) Samanta, A.; Fessenden, R. W. *J. Phys. Chem. A* **2000**, *104*, 8577.

(51) McCarthy, P. K.; Blanchard, G. J. *J. Phys. Chem.* **1993**, *97*, 12205.

(52) Rechthaler, K.; Köhler, G. *Chem. Phys.* **1994**, *189*, 99.

(53) Zerner, M. C.; Loew, G. H.; Kirchner, R. F.; Mueller-Westerhoff, U. T. *J. Am. Chem. Soc.* **1980**, *102*, 589.

(54) Frisch, M. J.; Trucks, G. W.; Schlegel, H. B.; Gill, P. M. W.; Johnson, B. G.; Robb, M. A.; Cheeseman, J. R.; Keith, T.; Peterson, G. A.; Montgomery, J. A.; Raghavachari, K.; Al-Laham, M. A.; Zakrewski, V. G.; Ortiz, J. V.; Foresman, J. B.; Cioslowski, J.; Stefanov, B. B.; Nanayakkara, A.; Challacombe, M.; Peng, C. Y.; Ayala, P. Y.; Chen, W.; Wong, M. W.; Andres, J. L.; Repogle, E. S.; Gomberts, R.; Martin, R. L.; Fox, D. J.; Binkley, J. S.; Defrees, D. J.; Baker, J.; Stewart, J. P.; Head-Gordon, M.; Gonzales, C.; Pople, J. A. *Gaussian 94*, revision E.2; Gaussian, Inc.: Pittsbugh, PA, 1995.

(55) Miller, K. J. *J. Am. Chem. Soc.* **1990**, *112*, 8533.

(56) Reynolds et al.[31] report both the direct measurements of the absorption and emission spectral moments and the solvent-components only. The latter was obtained from the deconvolution of the optical line with the line in 2-methylbutane, according to eq 54. This procedure assumes decoupling of the vibrational and solvent modes, which does not hold for C153. In our analysis, we used therefore the total experimental Stokes shifts and widths.

(57) Gustavsson, T.; Gulbinas, C. V.; Gurzadyan, G.; Mialocq, J.-C.; Pommeret, S.; Soegius, M.; van der Meulen, P. *J. Phys. Chem. A* **1998**, *102*, 4229.

(58) Matyushov, D. V.; Schmid, R. *J. Chem. Phys.* **1996**, *104*, 8627.

(59) A condensed phase dipole moment can be used in the perturbation scheme in eq 58 instead of the vacuum transition dipole.[60] If the dependence on the solvent configurations enters the transition dipole only through the instantaneous energy gap $\Delta E[\mathbf{R}_p]$, the δ-function in eq 55 replaces the solvent dependence with a corresponding power of $\bar{\nu}$. A $\bar{\nu}$-dependent, effective transition dipole then enters eq 59.[42] This fact, however, does not affect the necessity to include the dependence of the FC factor on the interaction term in eq 60 in cases of large transition dipoles solvated by polar solvents.

(60) Matyushov, D. V.; Voth, G. A. *J. Phys. Chem. A* **2000**, *104*, 6485.
(61) Matyushov, D. V. *J. Chem. Phys.* **2001**, *115*, in press.
(62) (a) Kakitani, T.; Mataga, N. *J. Phys. Chem.* **1985**, *89*, 8. (b) Fonseca, T.; Ladanyi, B. M.; Hynes, J. T. *J. Phys. Chem.* **1992**, *96*, 4085.
(63) Lambert, C.; Nöll, G. *J. Am. Chem. Soc.* **1999**, *121*, 8434.
(64) Nelsen, S. F. *Chem. Eur. J.* **2000**, *6*, 581.
(65) (a) Wang, C.; Mohney, B. K.; Williams, R. D.; Petrov, V.; Hupp, J. T.; Walker, G. C. *J. Am. Chem. Soc.* **1998**, *120*, 5848. (b) Wang, C.; Mohney, B. K.; Akhremitchev, B. B.; Walker, G. C. *J. Phys. Chem. A* **2000**, *104*, 4314. (c) Lobaugh, J.; Rossky, P. J. *J. Phys. Chem. A* **2000**, *104*, 899.
(66) Kovalenko, S. A.; Eilers-König, N.; Senyushkina, T. A.; Ernsting, N. P. *J. Phys. Chem. A* **2001**, *105*, 4834.
(67) (a) Wertheim, M. S. *Mol. Phys.* **1979**, *34*, 1109. (b) Joslin, C. G.; Gray, C. G.; Gubbins, K. E. *Mol. Phys.* **1985**, *54*, 1117.
(68) Matyushov, D. V.; Voth, G. A. *J. Chem. Phys.* **2000**, *113*, 5413.